Investigation of the Acyl Carrier Protein

Binding Partners SpoT and AidB

By

Julia L. Cottle

Submitted in partial fulfillment of the requirements
for the degree of Master of Science

at

Dalhousie University
Halifax, Nova Scotia
April 2010

DALHOUSIE UNIVERSITY

DEPARTMENT OF BIOCHEMISTRY AND MOLECULAR BIOLOGY

The undersigned hereby certify that they have read and recommend to the Faculty
of Graduate Studies for acceptance a thesis entitled "Investigation of the Acyl Carrier
Protein Binding Partners SpoT and AidB" by Julia L. Cottle in partial fulfillment of the
requirements for the degree of Master of Science.

Dated: _____

Supervisors: _____

_____

Readers: _____

_____

DALHOUSIE UNIVERSITY

DATE: April 23 2010

AUTHOR: Julia L. Cottle

TITLE: Investigation of the Acyl Carrier Protein Binding Partners SpoT and AidB

DEPARTMENT OR SCHOOL: Department of Biochemistry and Molecular Biology

DEGREE: M.Sc.   CONVOCATION: October   YEAR: 2010

"It takes all the running you can do, to keep in the same place"

The Red Queen from Lewis Carroll's
"Through the Looking-Glass"

Table of Contents

List of Tables

List of Figures

Abstract

Acyl carrier protein plays an essential role in bacterial fatty acid synthesis and has been recognized as an attractive new antibiotic target. In a previous study using TAP tagged ACP, we identified two ACP binding partners not directly involved in lipid metabolism, AidB and SpoT, that showed increased binding to ACP in stationary phase. In the current project, we found that the increase in binding of SpoT, a stringent response protein, to ACP appears to be due to increased affinity. In contrast, the increase in binding of AidB, an adaptive response protein, appears to be due to increased expression of AidB. Transformation of SpoT-TAP strains with pGEX-ACP vectors followed by purification revealed that SpoT interacts with wild type ACP, but not with ACP mutants that neutralized helix II or cannot fold properly. We used a far western approach to confirm the direct interaction between ACP and AidB in vitro. Overall, these results support the hypothesis that interaction of ACP with SpoT is highly specific and may reflect a regulatory role for ACP, while that with AidB might reflect non-specific interactions.

List of Abbreviations and Symbols Used

ACP	Acyl carrier protein
AcpH	ACP phosphodiesterase
AcpS	Holo-ACP synthase
Ada	Adaptive response protein: regulatory protein ada
AidB	Adaptive response protein: protein aidB
AlkA	Adaptive response protein: DNA-3-methyladenine glycosylase 2
AlkB	Adaptive response protein: alpha-ketoglutarate dependent dioxygenase alkB
BCA	Bicinchoninic acid
BSA	Bovine serum albumin
DTT	Dithiothreitol
E. coli	*Escherichia coli*
F50A	F50A mutant of *Vibrio harveyi* ACP
FAS I	Fatty acid synthase type I
FAS II	Fatty acid synthase type II
HRP	Horseradish peroxidase
IDA	Information dependent acquisition
IPTG	Isopropyl-D-1-thiogalactopyranoside
LB	Luria-Bertani
MNNG	N-methyl-N'-nitro-N-nitrosoguanosine
MRM	Multiple reaction monitoring

MRSA	Methicillin-resistant *Staphylococcus aureus*
MS	Mass spectrometry
OVA	Ovalbumin
pI	Isoelectric point
(p)ppGpp	guanosine penta/tetraphosphate
PsI	alernative name for RelA, (p)ppGpp synthetase
PsII	alernative name for SpoT, (p)ppGpp synthetase/hydrolase
RelA	(p)ppGpp synthetase
RSH	GTP pyrophosphokinase rsh
SA	Site A mutants on helix II of *V. harveyi* ACP
SA/SB	Site A and site B mutants on helix II of *V. harveyi* ACP
SB	Site B mutants on helix II ACP
SDS	Sodium dodecyl sulfate
Ser-36	Serine 36
SPA	Sequential peptide affinity
SpoT	(p)ppGpp synthetase/hydrolasae
Staph. aureus	*Staphylococcus aureus*
TAP	Tandem affinity purification
TB	Terrific broth
TEV	Tobacco etch virus
V. harveyi	*Vibrio harveyi*
VRSA	Vancomycin-resistant *Staphylococcus aureus*

Acknowledgements

I first and foremost would like to thank Drs. David Byers and Chris McMaster for their direction and patience. Without their continued support and guidance I would not have been able to persevere through the turbulent adventures of scientific research. I owe many thanks to Elden Rowland at the Proteomics Core Facility, who undoubtedly worked with me on parts of my project and continues to share with me his knowledge and insight. I would also like to thank the other members of the Byers and McMaster Labs. In particular I would like to extend my gratitude towards Peter Murphy, Anne Murphy, Pedro Fernandez-Murray, and Marissa LeBlanc. I am also very appreciative for the valuable suggestions and advice given to me by my third committee member Dr. Rick Singer over the past few years.

Chapter I: Introduction

A. Antibiotic Targets in Lipid Metabolism

Infectious disease is the second leading cause of death worldwide, and the third leading cause of death in North America, behind only heart disease and cancer (Pinner, Teutsch et al. 1996). The incidence of infectious disease is on the rise. In the United States, bacteria are the most frequent cause of infectious disease-related deaths (Infectious Disease Society of America 2004). Antibiotics have been used to treat many people with infectious disease over the past 65 years and have increased life expectancy dramatically (Infectious Disease Society of America 2004). Unfortunately and inevitably, bacteria have developed resistance to both single and multi-drug regimes. Bacterial resistance has been an issue since the introduction of the first antibacterial agents (Powers 2004). Infections that were once easily treated with antibiotics are becoming more of a challenge (Infectious Disease Society of America 2004). A recent example is the report of a vancomycin-resistant *Staphylococcus aureus* (VRSA) in June 2002. Due to its toxicity, vancomycin is seen as a last resort antibiotic most often targeted towards the nosocomial strains of methicillin-resistant *Staph. aureus* (MRSA). Resistance can complicate treatment of bacterial infections in clinical settings and subsequently increase mortality rates (Slama 2008). A recent review of 21 original studies concluded that gram-negative bacterial resistance increases the burden on healthcare systems, by the resulting increased hospital stay and costs (Shorr 2009). Examination of the US Food and Drug Administration's history of antibiotic approvals reveals that there have been,

problematically, no new classes of antibiotics introduced since the 1960s (Powers 2004). The decrease in the number of effective antibiotics for treatment of constantly adapting infectious diseases suggests an urgent need for new classes of antibiotics with novel mechanisms (Spellberg, Powers et al. 2004).

There are at least two qualities that new drug targets should have. First, it is important that the new target differs between eukaryotes and prokaryotes, so that its inhibitors do not affect human cellular function. Secondly, the particular target should be essential so as to stop growth or kill bacterial cells. A third beneficial feature of an antibiotic target would be conservation across multiple bacterial species, resulting in the possibility of a broad spectrum antibiotic.

Recently, research has focused on lipid biosynthesis as a target for antibacterial compounds (Heath, White et al. 2001). This has been encouraged by efforts to catalog three-dimensional structures of the majority of the enzymes involved in fatty acid synthesis (White, Zheng et al. 2005). In bacteria there is a high degree of conservation among many proteins involved in lipid metabolism, making them attractive targets for the development of broad-spectrum antibiotics (Wright and Reynolds 2007). Moreover, lipid metabolism differs in eukaryotes and prokaryotes, and involves many essential enzymes, yet has been largely unexplored for its antibiotic potential (Wright and Reynolds 2007). Some of the targets currently being examined include, but are not limited to: fatty acid synthesis, lipid A biosynthesis, and phospholipid synthesis (Heath, White et al. 2001). As the hydrophobic component of phospholipids, fatty acids are central for the formation of lipid membranes. Some of the enzymes involved in fatty acid synthesis have been the focus for antibacterial drug development for decades (Heath, White et al. 2001).

Triclosan and isoniazid are two antibiotics in use that disrupt bacterial fatty acid synthesis.

In mammals, type I fatty acid synthase (FAS I) is a homodimer of a large multifunctional protein subunit of about 2 500 residues (Smith, Witkowski et al. 2003). In prokaryotes, type II fatty acid synthase (FAS II) is made up of a series of discrete proteins that catalyze each step individually in the biosynthetic pathway. The regulation of FAS II is tightly controlled to ensure synchronization of fatty acid production with lipid membrane synthesis and cell growth (Jiang and Cronan 1994). FAS II from *Escherichia coli* has been extensively characterized and three dimensional structures of all component enzymes have been elucidated (White, Zheng et al. 2005). Even though reactions catalyzed by both FAS I and FAS II are similar, the differences in enzyme structure and the essential nature of the proteins involved in FAS II allow for the development of new target-specific antibacterial drugs (Campbell and Cronan 2001, Zhang, White et al. 2006).

The central component of both FAS I and FAS II is acyl carrier protein (ACP), and its different structure and mechanism in both these processes make it an exciting antibacterial target. Each subunit of FAS I contains ACP as a central domain, and its strategic location in the multifunctional protein gives it access to all the other enzyme components. FAS I ACP is restricted primarily to de novo synthesis of fatty acids. On the other hand, ACP in FAS II is found as a discrete, soluble protein. Acyl group intermediates remain covalently attached to ACP, which acts like a shuttle as it delivers fatty acids among active sites during fatty acid elongation (Heath, Jackowski et al. 2002) (Figure 1). The majority of the fatty acids produced in *E. coli* have 16 or 18 carbons and
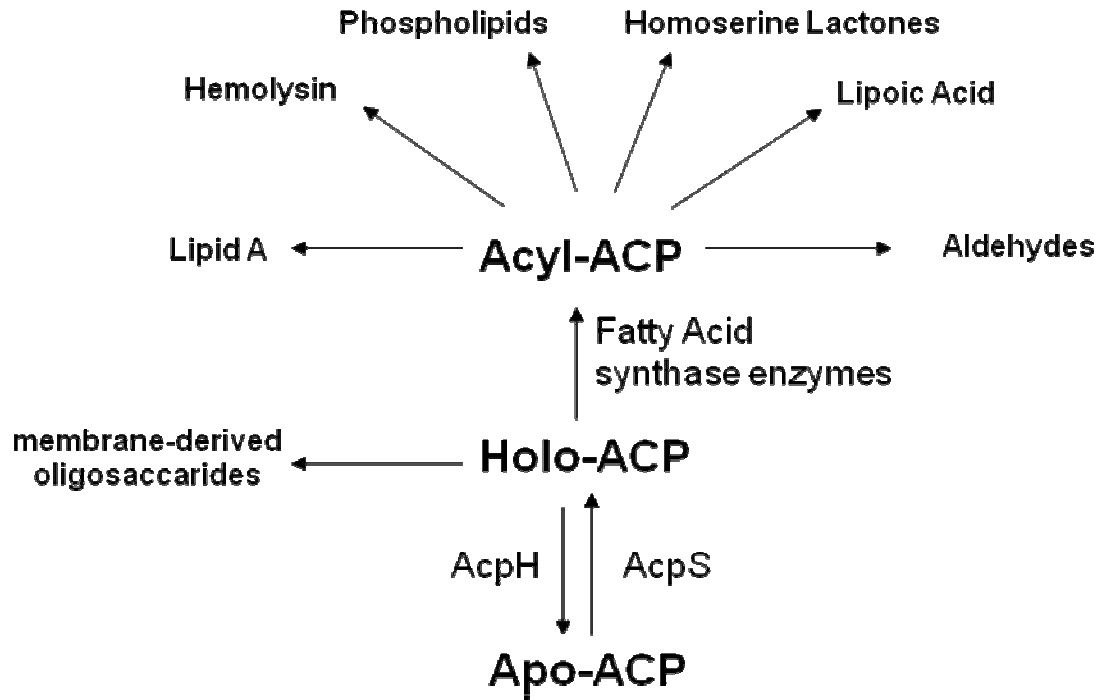
Figure 1: ACP-dependent pathways in Gram negative bacteria. ACP is expressed from the *acpP* gene as apo-ACP and then modified by the addition of a phosphopantetheine group by ACP synthase (AcpS) to form holo ACP. ACP phosphodiesterase (AcpH) converts holo-ACP to apo-ACP. The active holo-ACP can be converted to various acyl-ACP derivatives during fatty acid synthesis, and are used to make numerous products in the cell. These various forms of ACP are binding partners of many of the enzymes involved in the production of the products seen in the figure.

are mainly directed to the inner membrane and the inner leaflet of the outer membrane as phospholipids. Bacterial acyl-ACPs are also directly used as acyl donors for phospholipid synthesis, while mammalian FAS I produces free fatty acids which must be activated to acyl-CoAs for further elongation or degradation (Rock and Jackowski 1982).

B. Structure and Function of Bacterial ACP

ACP is an essential protein for bacterial growth and pathogenesis, contributing to the synthesis of many lipid products (Figure 1). It is one of the most abundant proteins in *E. coli*, constituting approximately 0.25% of the bacteria's total soluble protein (Rock and Cronan, 1979). It is also remarkably small, ranging from 70 to 100 amino acids in length. ACP functions to provide acyl groups for biosynthesis of phospholipids (Rock and Cronan 1996), lipid A (Anderson and Raetz 1987), homoserine lactones (Issartel, Koronakis, et al. 1991), lipoic acid (Jordan and Cronan 1997), membrane-derived oligosaccharides (Therisod, Weissborn et al. 1986), and hemolysin (Hughes, Issartel et al. 1992), as well as being a source of the aldehyde substrate of luciferase in bioluminescent bacteria such as *Vibrio harveyi* (Byers and Meighen 1985).

Comparisons of over 250 bacterial genome sequences suggest a significant level of primary structure conservation among bacterial ACPs. The similar nature of ACPs becomes even more apparent when comparing three dimensional structures (Byers and Gong 2007). All ACPs exhibit a similar four helix bundle structure that can encase the
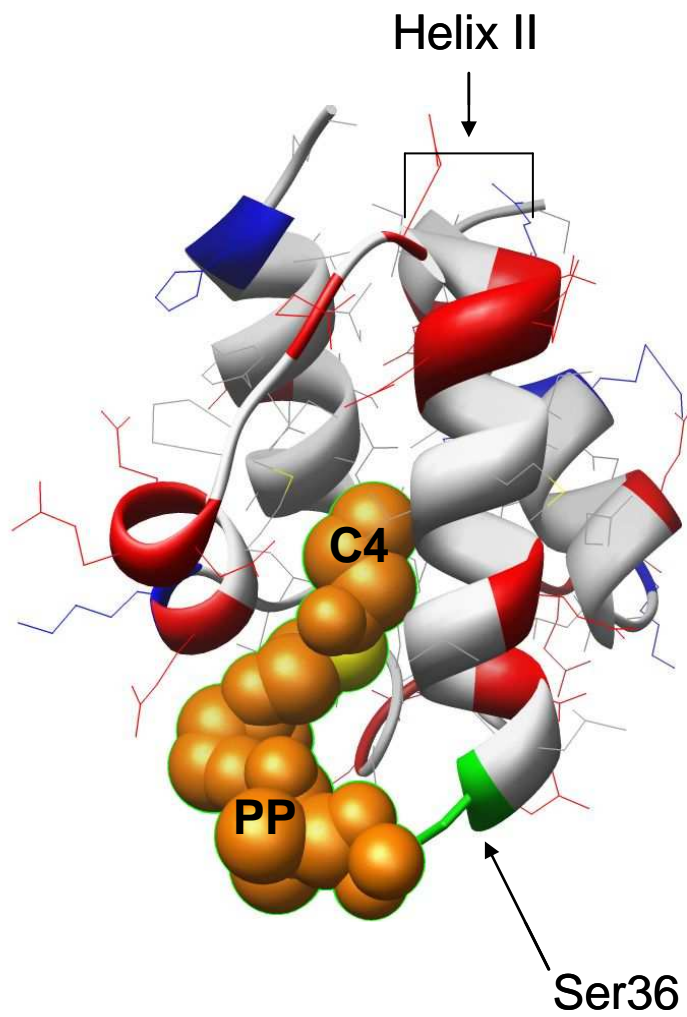
Figure 2: *E. coli* butyryl(C4)-ACP. The polypeptide chain is shown as a ribbon, while the acyl-phosphopantetheine (PP) is in a space-fill representation. Acidic and basic residues are colored red and blue, respectively, while Ser-36 at the beginning of helix 2 is green.

attached fatty acyl chain. In *E. coli* these helices make up 50% of the secondary structure of ACP (Kim and Prestegard 1990) (Figure 2). Helix II is among the most highly conserved regions of ACP; this very acidic region is implicated in binding many of the partner enzymes of ACP through electrostatic interactions (Zhang, 2001).

An important characteristic of ACP is the modification of the *acpP* gene product apo-ACP to its functional form, holo-ACP. The majority of ACP found in the cell is in the active holo form (Rock and Jackowski, 1982). This post-translational modification is catalyzed by ACP synthase (AcpS), which attaches a 4'-phosphopantetheine prosthetic group to the highly conserved serine-36 near the N terminal end of helix II. This enzymatic reaction is currently of great interest as a drug target, as virtually all functions of ACP require this modification. The isolation of a natural product with antibacterial activity inhibiting AcpS has promoted continued attention to this target (Chu, Mierzwa et al. 2003).

The fatty acyl chain is covalently attached to the phosphopantetheine sulfhydryl group of holo-ACP through a thioester bond. Acyl-ACPs represent only a small portion of the total ACP pool under normal steady state conditions (Rock and Jackowski 1982). These fatty acyl chains are shuttled from one enzyme to another by ACP. Many acyltransferases also bind selected acyl-ACP intermediates with specific fatty acyl chain lengths. For example, four acyltransferases involved in the sequential, chain length specific attachment of fatty acids to lipid A, an endotoxin found on the external leaflet of the outer membrane, bind *E. coli* acyl-ACPs with a length of 12 - 14 carbons (Raetz, Reynolds et al., 2007). The fatty acid specificity of enzymes for acyl-ACP substrates

suggests that there are significant characteristics associated with chain length which are important for protein binding and/or reaction.

Upon fatty acylation holo-ACP maintains its overall secondary structure, while shifting the ACP to a more compact and ordered state (Jones, Holak et al. 1987). The structural stability provided by acyl chain enclosure can be affected by site-directed mutagenesis of residues in a putative fatty acid binding pocket of ACP (e.g. Phe-50 and Ile-54). ACP mutants in which Phe-50 or Ile-45 are replaced by Ala are unable to fold properly. Work from our laboratory has shown that the F50A mutation most likely decreases the stability of fatty acyl binding through a conformational change resulting in an unfolded protein (Flaman, Chen et al. 2001) (Figure 3A). *E. coli* ACP has relatively greater conformational stability than *V.harveyi* ACP and, unlike the latter, is folded at neutral pH. This is thought to be due to the presence of a basic histidine residue at the C-terminus of the former protein (Keating, Gong et al. 2002). These characteristics could reflect the requirement of ACP to undergo reversible conformational change for its primary functional roles of binding, carrying, and releasing acyl groups in multiple enzyme pathways (Byers and Gong 2007).

With a pI of approximately 4, *E. coli* ACP is composed of 26% acidic residues and only 8% basic residues, most of which are located near the N- and C- termini. The acidic nature of ACP results in electrostatic repulsion that contributes to the inherent flexibility of ACP (Byers and Gong, 2007). Due to this acidic character, ACP appears to belong to a family of natively unfolded proteins, which although capable of being unstructured under physiological conditions are functional (Wright and Dyson 1999). ACP flexibility was originally shown by the existence of two conformational isoforms in
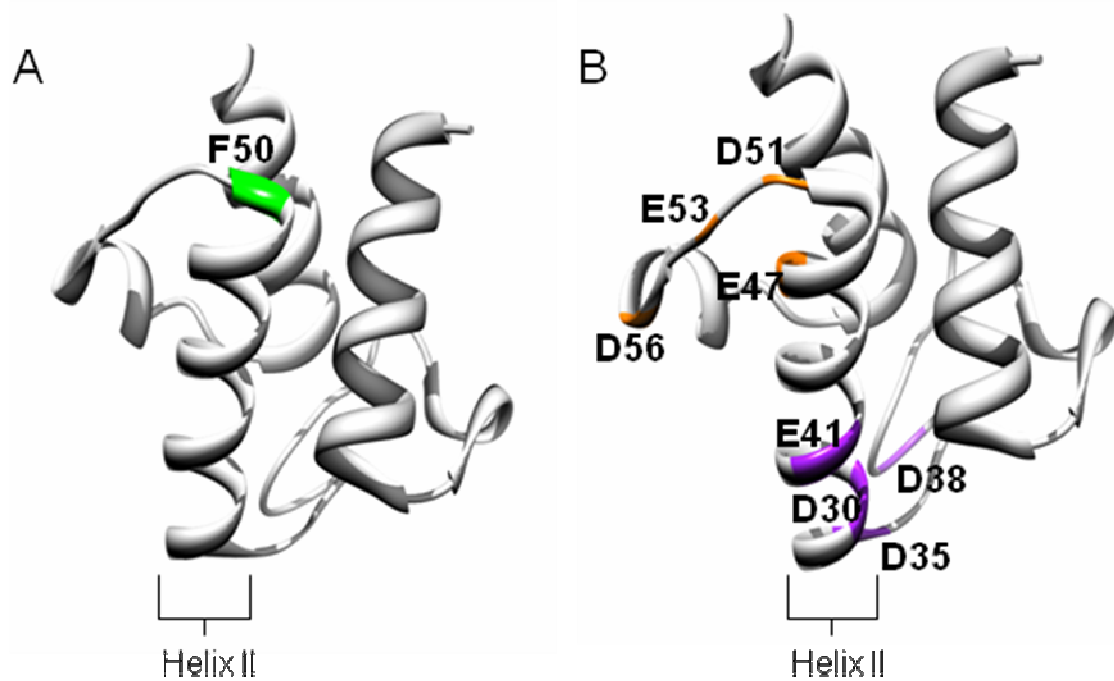
Figure 3: Mutations that affect ACP function. The polypeptide chain of *E. coli* butyryl(C4)-ACP is shown as a ribbon in both panel A and B. In panel A the amino acid residue Phe 50 is identified in green, seen at the top of helix II; this is the site of the F50A mutation that prevents ACP from folding. In panel B the four amino acid residues of divalent cation-binding sites A and B are marked. Site B residues are in orange, while site A residues are in purple. Figures were made in Chimera (alpha version 1.3) and rendered in POV-Ray (Version 3.6) from the PBDID file 1L0H.

NMR studies for *E. coli* and spinach ACP (Kim and Prestegard 1990). NMR has also

shown that loop I, helix II, and helix III of ACP have the greatest mobility (Kim,

Kovrigin et al. 2006). The binding of some divalent cations neutralizing the acidic

residues in helix II has also been shown to stabilize ACP (Tener and Mayo 1990). On

both ends of helix II there are low affinity cation binding sites consisting of clusters of

acidic residues, termed site A and site B. (Figure 3B). Site A is found at the N-terminal

region of helix II (residues 35-41) and site B at the opposite end of helix II (residues 47-

56) (Gong, Murphy et al. 2007). Both LpxA and AcpS interactions with *V. harveyi* ACP

are affected by site A and site B mutations that neutralize these acidic residues (Flaman,

Chen et al. 2001; Gong, Murphy et al. 2007). ACP conformation is not radically affected

by the mutation of just one of these sites, but mutagenic neutralization of both sites

stabilizes ACP conformation in the absence of divalent cations at neutral pH (Gong,

Murphy et al. 2007).

Despite its small size, ACP is one of the most promiscuous protein binding

partners in *E. coli* (Butland, Peregrin-Alvarez et al. 2005). With no common ACP-

binding motifs apparent in ACP binding partners, the acidic nature of ACP in large part

provides the basis for interaction with basic regions on its partner enzymes (Gould,

Schweizer et al. 2004). Indeed, basic regions have been identified on several enzymes in

E. coli FAS II that are assumed to form electrostatic interactions with acidic helix II of

ACP (Zhang, Rao et al. 2001). This has prompted helix II to be named the `recognition`

site of ACP (Zhang, Wu et al. 2003). The role of helix II was first revealed from the

structure of ACP complexed with holo-acyl carrier protein synthase (AcpS) from *Bacillus*

subtilis (Parris, Lin et al. 2000). The importance of these acidic residues has been further

established through site-directed mutagenesis, resulting in decreased binding with partner

enzymes (Gong, Murphy et al. 2007). Despite this general theme, mutagenesis has

different effects on ACP partner enzymes, suggesting some fine tuning of these

interactions (Gong, Murphy et al. 2007, Flaman 2001). With different enzymes binding

different regions of helix II, their locations may give us insight on activity or information

transferred.

C. ACP Binding Partners

As noted above, recent proteomic studies suggest that ACP is a promiscuous

protein interacting with over three dozen proteins in *E. coli*, over one third of which have

no obvious involvement in lipid metabolism (Butland, Peregrin-Alvarez et al. 2005). The

development of stringent affinity purification procedures, such as tandem affinity

purification (TAP) and sequential peptide affinity (SPA), coupled with mass

spectrometry, has facilitated the isolation and analysis of protein complexes (Butland,

Peregrin-Alvarez et al. 2005). Both TAP and SPA tags introduce a dual affinity cassette

to the N or C terminus of the protein of interest by site-specific recombination (Figure 4).

The incorporation of the tagged gene within the genome under its natural promoter

enables gene expression and protein interactions to occur at endogenous levels, thus

avoiding non-specific binding which is common when one partner is overexpressed.

Using TAP and SPA protocols illustrated in Figure 5, Toronto based researchers

identified over 30 ACP binding partners, including but not limited to some obvious

binding partners with a known direct involvement in lipid metabolism
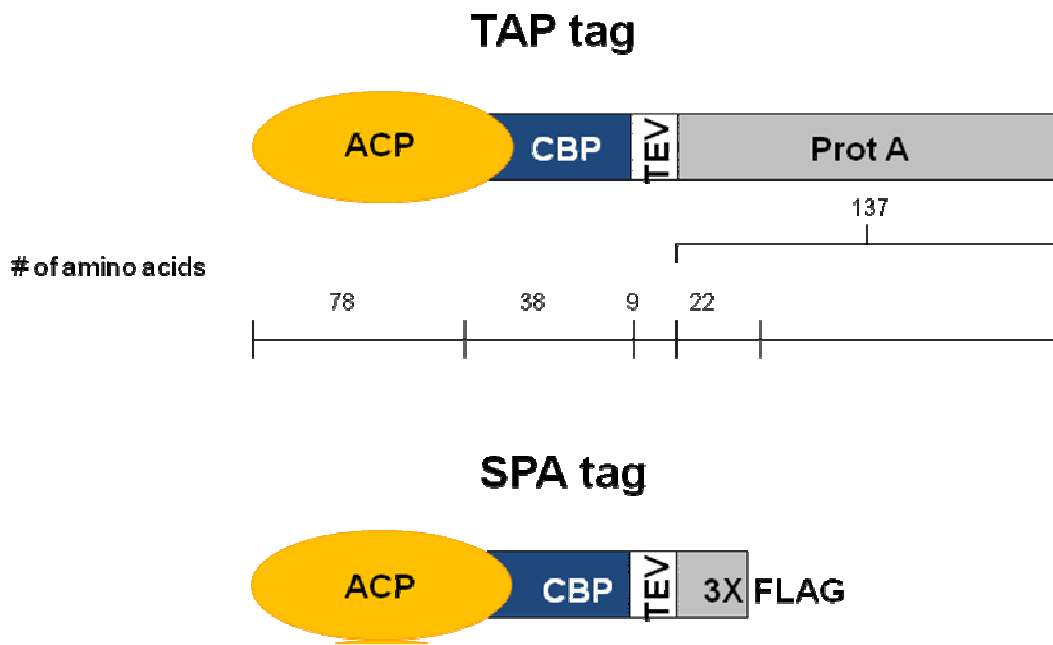
Figure 4: Schematic diagram of ACP with a C-terminal TAP tag and a C-terminal SPA tag. The target protein, ACP, has been fused with the C-terminal TAP tag composed of a calmodulin binding peptide (CBP), *Tobacco Etch Virus* protease cleavage site (TEV), and two IgG domains of protein A (ProtA). The SPA tag is composed of calmodulin binding peptide (CBP), *Tobacco Etch Virus* protease cleavage site (TEV), and 3X Flag domain.
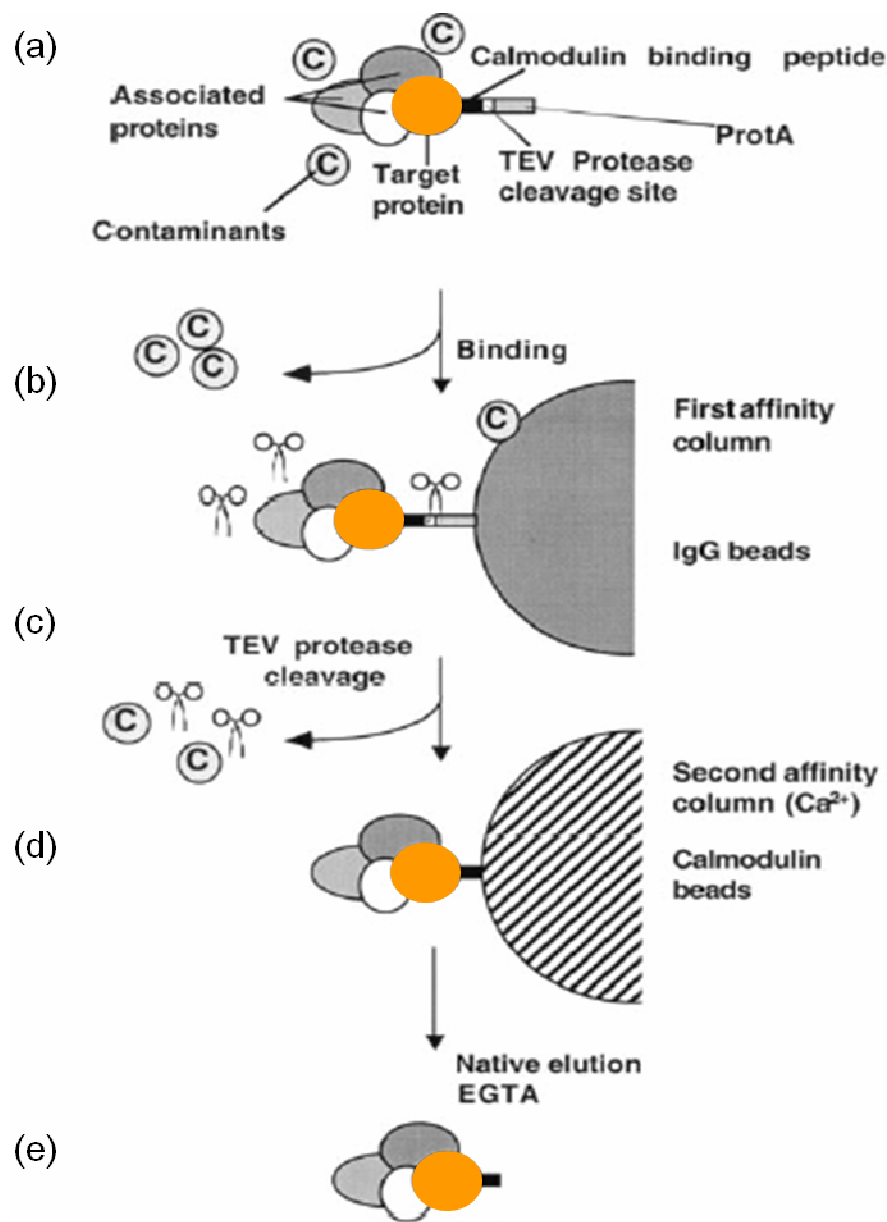
Figure 5: Overview of the TAP tag purification method. (a) The target protein with the C-terminal TAP tag associates with other proteins under native conditions. Cells are lysed and (b) the complex containing the bait protein with the protein A moiety is retained on IgG beads. (c) Cleavage by TEV protease at the cleavage site releases the complexes. (d) The second purification step involves the binding of the CBP moiety to calmodulin beads in the presence of Ca^{2+}. (e) The target protein and its binding partners are then eluted with EGTA (adapted from Puig et al., 2001).

(Butland, Peregrin-Alvarez et al. 2005). Although some of these interactions have been

independently verified using bacterial two-hybrid systems, reciprocal tagging and split

affinity tags, it is possible that other interactions may be a result of electrostatic attraction

to ACP. Many of the interactions have yet to be fully characterized.

In my Honours project, conducted in the Byers laboratory, I used similar

approaches to identify numerous ACP binding partners including several identified

previously by Butland et al. (2005) (Table 1), as well as potential new partners including

MukE and MukF (Figure 6). While examining ACP-TAP binding partners under various

growth conditions it was noted that interaction with some binding partners was growth

phase dependent. Specifically, there was an increase in the amount of the proteins SpoT

and AidB purified with ACP-TAP in stationary phase (Figure 7). SpoT, a dual function

ppGpp synthetase and hydrolase, is involved in the cellular stress response to nutrient

deficiencies while AidB, an adaptive response protein, is involved in the response to

alkylation damage of DNA. How these environmental stress responses and lipid

metabolism may be connected through ACP is still not understood.

D. (p)ppGpp Synthetase and Hydrolase (SpoT)

SpoT is an enzyme in *E. coli* and other bacteria involved in the cell retort to

environmental stress called the stringent response. The stringent response is the bacterial

reaction to nutrient starvation and is associated with the onset of stationary phase in many

bacteria. It involves the control of gene expression and a resulting decrease in metabolic

activity through an accumulation of guanosine penta/tetraphosphate ((p)ppGpp),

ACP-TAP co-purified proteins	Protein Name	*E. coli* pI
AcpP	acyl carrier protein	3.89
Aas	2-acylglycerophosphoethanolamine acyl transferase-acyl-acyl carrier protein synthetase: long chain fatty acid CoA ligase	9.31
AcpS	holo-ACP synthase: transfers the 4'-phosphopanteteine moiety from CoA to a Ser on ACP	9.30
AidB	adaptive response protein	7.98
FabB	3-oxoacyl-ACP synthase: involved in FAS II	5.35
FabF	3-oxoacyl-ACP synthase: involved in FAS II	5.71
FabG	3-oxoacyl-ACP reductase: involved in FAS II	6.76
FabH	3-oxoacyl-ACP synthase III: involved in FAS II	5.08
FabZ	(3R)-hydroxymyristoyl-ACP dehydratase: involved in FAS II	6.84
GlmU	bifunctional protein (i) UDP-N-actylglucosamine pyrophorylase (ii) glucosamine 1-phosphate N-acyltransferase: catalyzes last two sequential reactions in de novo UDP-GlcNAc biosynthetic pathway	6.09
IscS	cysteine desulfurase: alanine biosynthesis III	5.94
LpxA	UDP-N-acetylglucosamine acyltransferase: involved in Lipid A biosynthesis	6.63
LpxD	UDP-3-O-(3-hydroxymyristoyl) glucosamine N-acyltransferase: involved in Lipid A synthesis	6.07
MukB	chromosome partition protein mukB	5.24
MukE	chromosome partition protein mukE	4.92
MukF	chromosome partition protein mukF	4.75
PlsB	glycerol-3-phosphate acyltransferases	8.51
RibF	riboflavin biosynthesis protein: kinase and FMN adenylyltransferase	9.34
RplD	50S ribosomal protein L4	9.72
RplO	50S ribosomal protein L15	11.15
RpsC	30S ribosomal protein S3	10.27
RpsD	30S ribosomal protein S4	10.05
RpsE	30S ribosomal protein S5	10.11
RpsG	30S ribosomal protein S7	10.36
SpoT	bifunctional (p)ppGpp synthetase and hydrolase	8.89
YbgC	acyl-CoA thioester hydrolase	6.91
YiiD	uncharacterized protein with an acetyltransferase domain	5.92

Table 1: Proteins co-purified with ACP-TAP (with pI of the partner proteins). The ACP-TAP eluate was separated by SDS-PAGE and the individual protein bands were analyzed by MS/MS.
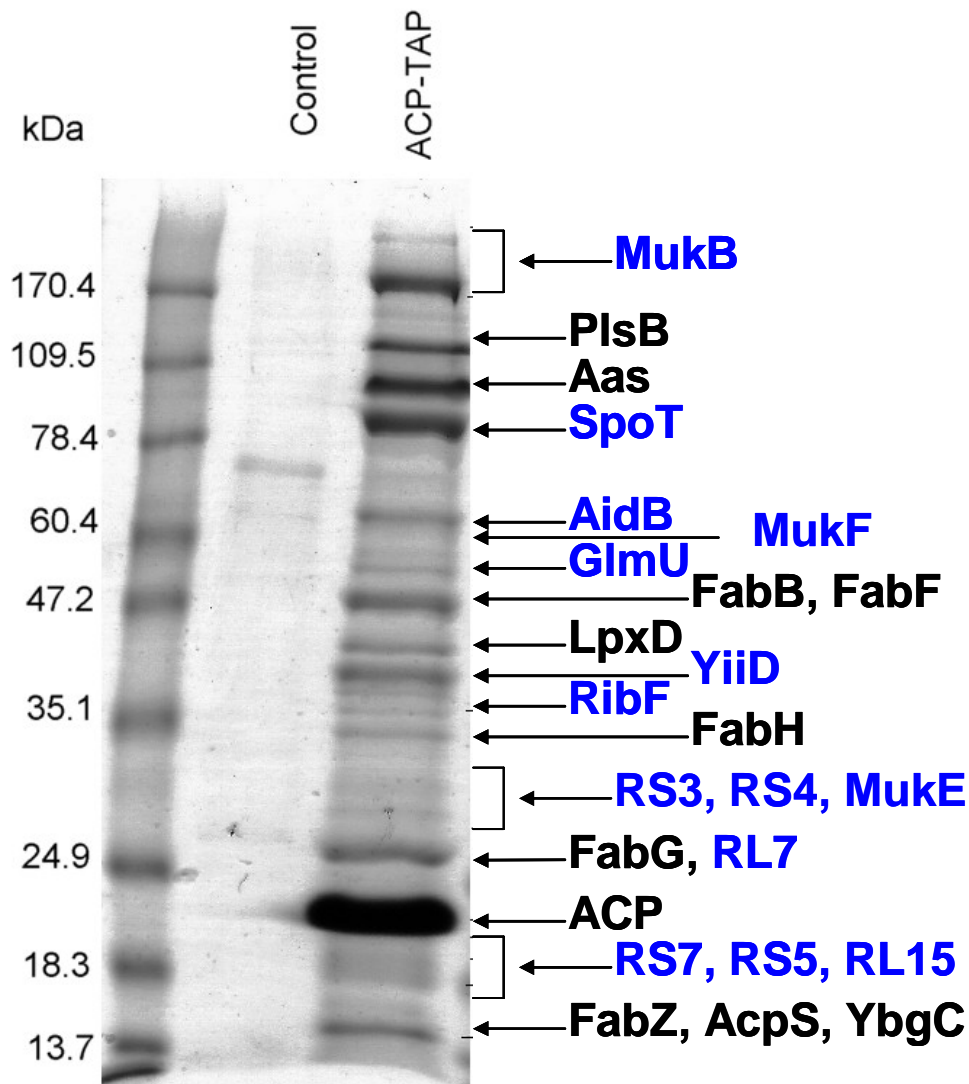
Figure 6: ACP-associated proteins isolated using the ACP-TAP system. Proteins labeled in black have a known connection to bacterial lipid metabolism, while the proteins labeled in blue do not have an obvious connection. ACP-TAP or control (DH5α) cells were grown in 500 mL of TB at 30ºC to an A_{660} of approximately 1.0, proteins were isolated using the original TAP purification procedure. Acetone was removed through centrifugation at 15 000 rpm for 15 minutes. The pellet was resuspended in 20 µL of 1X SDS and 1 mM DTT and the presence of the proteins were verified using 15 % SDS-PAGE and stained with GelCode Blue stain. Standard in lane 1 is BenchMark Pre-Stained Protein Ladder (Invitrogen). Labeled proteins were identified by tandem mass spectrometry and MASCOT analysis using the Swissprot database. (from J. Cottle, Hons project)
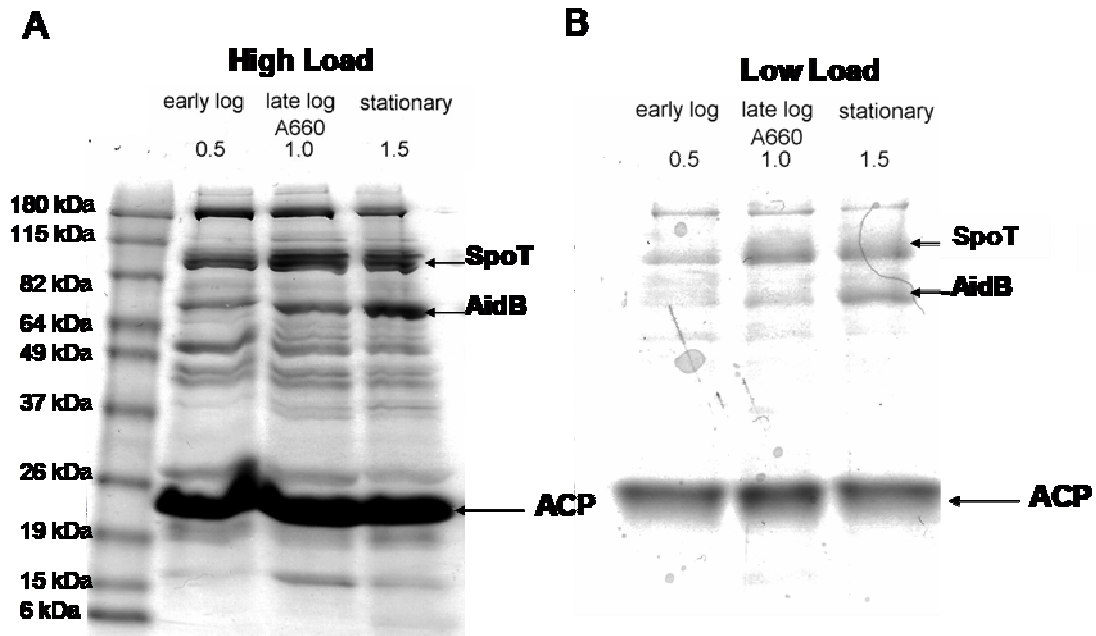
Figure 7: Growth stage dependent binding of proteins to ACP-TAP. (A) SDS-PAGE of proteins isolated from *E. coli* DH5α control and *E. coli* DH5α ACP-TAP at different growth stages. Cells were harvested during early log phase ($OD_{660} = 0.5$), late log phase ($OD_{660} = 1.0$), and stationary phase ($OD_{660} = 2.0$) as indicated. Proteins labelled are those that exhibited a change in band intensity as a function of growth. (B): SDS-PAGE analysis of different growth phases of *E. coli* DH5α ACP-TAP at a lower protein load to visualize the more abundant proteins. (from J. Cottle, Hons project)

termination of RNA synthesis, and activation of numerous stress response genes. SpoT is a member of the RSH enzyme superfamily, which is responsible for the synthesis and breakdown of the "alarmone" (p)ppGpp. When induced, (p)ppGpp affects bacterial physiology by inhibiting protein expression and cell growth (Svitil, 1993). Bacteria appear to have either a single RSH protein, often designated RelA, or two related RSH proteins, designated RelA and SpoT; in some literature these proteins are called PSI and PSII, respectively (Potrykus and Cashel 2008).

   E. coli contains both RelA and SpoT proteins. RelA is a pentaphosphate ((p)ppGpp) synthetase activated by the accumulation of uncharged tRNA molecules when cells undergo amino acid starvation (Wendrich, Blaha et al. 2002). By binding RNA polymerase, (p)ppGpp affects the transcriptional initiation of specific genes either positively or negatively (Paul, Barker et al. 2004). The (p)ppGpp produced by RelA is next hydrolyzed to ppGpp, which is believed to alter RNA polymerase affinity for various promoters (Chatterji, 2001). SpoT, homologous to RelA, is a dual-function enzyme with both (p)ppGpp synthetase activity and hydrolase activity (Hernandez and Bremer 1991). Unlike RelA, the synthetase activity of SpoT responds to phosphate starvation (Bougdour and Gottesman 2007). Both RelA and SpoT are found associated with ribosomes (Heinemeyer and Richter 1977). SpoT is conditionally essential: *E. coli* cells cannot grow when SpoT is deleted due to an accumulation of (p)ppGpp from RelA, but when both SpoT and RelA are deleted the cells survive (Xiao, Kalman et al. 1991). Even a small amount of SpoT appears to be sufficient for breaking down large quantities of (p)ppGpp involved in the stringent response (Sarubbi, Rudd et al. 1989). Recently it has been suggested that cellular changes due to the effects of (p)ppGpp accumulation

allow some bacteria to flourish within both general and niche-specific host environment (Wells and Gaynor 2006). The stringent response of the gram negative bacteria *Campylobacter jejuni*, with a single *Rsh* gene designated *spoT,* is important for survival not only in a general stationary phase but for the species-specific stress of lower carbon dioxide and/or higher oxygen levels (Gaynor, Wells et al. 2005).

Mutational analysis of *E. coli spoT* identified two distinct regions, each responsible for one of the two enzymatic activities of SpoT. The N-terminal 203 residues of the total 702 are sufficient for (p)ppGpp synthetase activity, while an overlapping region (residues 67-374) is sufficient for (p)ppGpp hydrolase activity (Cashel and Gentry 1996). The C-terminal half of SpoT is involved in the regulation of both activities (Gropp, Strausz et al. 2001; Mechold, Murphy et al. 2002). Relatively close to the center of the protein is the TGS domain, so named as it has been found in threonyl-tRNA synthetase, GTPases, and SpoT (Wolf, Aravind et al. 1999).

E. Acp and SpoT Interaction

The interaction between ACP and SpoT has been verified as specific, as it does not occur with RelA or with a non-functional (S36A) mutant of ACP (Battesti and Bouveret 2006). SpoT bears some sequence homology to AcpH, an ACP phosphodiesterase that is responsible for the turnover of the 4'phosphopantetheine group by hydrolyzing the active holo-ACP to the non-active apo-ACP (Thomas, Rigden et al. 2007). This suggests a possible shared interaction site or other functional features involved in the interaction with ACP (Byers and Gong 2007). An increase in the

19

alarmone (p)ppGpp has also been shown to block expression of FAS II genes as well as inhibit PlsB activity, the rate-limiting step in phospholipid synthesis (DiRusso and Nystrom 1998). Lipid metabolism involvement in SpoT regulation has also been suggested because of increased (p)ppGpp levels in relA⁻ strains exposed to cerulenin, a FAS II inhibitor (Seyfzadeh, Keener et al. 1993). SpoT mutations that prevent the SpoT-dependent (p)ppGpp accumulation in response to cerulenin also do not interact with ACP (Battesti and Bouveret 2006). Battesti and Bouveret (2006) have also recently shown that ACP interacts with SpoT at the central TGS domain. There is also a very similar TGS domain in RelA, but the N-terminal domain of RelA may prevent ACP from interacting with this TGS domain. This interaction site is consistent with ACP having a role in regulating SpoT activity. As noted above, holo-ACP, but not apo-ACP (S36A mutant), binds SpoT suggesting that SpoT may monitor the holo/acyl-ACP status of the cell. When ACP binds the TGS domain of SpoT, (p)ppGpp synthetase activity is turned off and basal hydrolase activity is turned on, counteracting the (p)ppGpp synthesis by RelA and maintaining a low level of (p)ppGpp in the cell. It is possible that accumulation of the acyl-ACP intermediates bound to SpoT could signal a state of nutritional deficiency in the cell through allosterically activating the SpoT synthetase to produce (p)ppGpp and thereby inhibit lipid metabolism (Battesti and Bouveret 2006).

F. AidB and Other Adaptive Response Proteins

The adaptive (Ada) response is an inducible DNA repair strategy to counteract the cytotoxic and mutagenic effects of alkylation agents found endogenously and in the

environment (Sedgwick and Lindahl 2002). DNA damaged through alkylation affects the stability of the genome (Bowles, Metz et al. 2008). In *E. coli* the adaptive response involves the induction and expression of four genes, *ada, alkA, alkB,* and *aidB* (Lindahl, Sedgwick et al. 1988)*. Ada* and *alkB* are found in an operon, while *alkA* and *aidB* are individually expressed. Ada, AlkA, and AlkB have all been functionally and structurally characterized (Samson and Cairns 1977; Sedgwick 2004), while the DNA repair mechanism of AidB is not as well characterized.

The Ada protein acts as a transcriptional activator of all four adaptive response genes, including its own. This multifunctional protein also shows methyltransferase activity (Teo, Sedgwick et al. 1984). The 39 kDa protein has two functionally independent domains: a 19 kDa C-terminus and a 20 kDa N-terminus. The C-terminal domain transfers a methyl group from the modified DNA onto its Cys-321 residue, which is then passed to Cys-36 on the N-terminal domain. Ada induces the expression of the adaptive response proteins in two different ways. For the *ada-alkB* operon and the *aidB* gene, the methylated N-terminal domain of Ada interacts with the α subunit of RNA polymerase, while the C-terminal domain interacts with the σ subunit. For the *alkA* gene, the N-terminal domain interacts with both the α and σ subunits and might not require methylation (Landini and Volkert 2000). The alkyation of Ada is irreversible, so the way in which the adaptive response is terminated is still unknown.

AlkA functions as a glycosylase, repairing a diverse group of methylated DNA bases (Lindahl, Sedgwick et al. 1988). Once the damaged DNA is recognized, AlkA repairs it by excising the methylated base (Hollis, Ichikawa et al. 2000) through cleavage of the bond to the DNA backbone (Hollis, Lau et al. 2001). AlkA has two domains with a

intervening catalytic region containing an essential aspartic acid (Labhan, Scharer et al. 1996). The modified base flips out of the DNA helix and into this catalytic region, resulting in distortion of the DNA (Hollis, Ichikawa et al. 2000).

AlkB is the product of the *alkB* gene, which is part of the *ada-alkB* operon induced by a methylated Ada protein. AlkB repairs single stranded DNA lesions resulting from S_N2 methylating agents (Dinglay, Trewick et al. 2000). As a member of the α-ketoglutarate-Fe^{2+}-dependant-dioxygenase superfamily, AlkB requires Fe^{2+} as a cofactor (Aravind and Koonin 2001). In the presence of α-ketoglutarate, it uses dioxygenase activity to directly demethylate adenine and cytosine, releasing the methyl group as formaldehyde (Falnes, Johansen et al. 2002). Methylated guanosine and thymine are also repaired by AlkB, but at a much lower rate (Koivisto, Duncan et al. 2003). If *alkB* is damaged or mutated the bacterial cells develop a greater sensitivity to alkyation damage (Nieminuszczy and Grzesiuk 2007).

G. AidB and ACP

The induction of AidB is similar to that of the other adaptive response proteins, involving methylated Ada protein binding to its regulatory region (Landini, Hajec et al. 1994). Methylated Ada is sufficient for the induction of *ada* and *alkB* expression (Nakabeppu and Sekiguchi 1986), but for *aidB* induction another factor appears to be necessary, as methylated Ada is only able to induce expression of *aidB* in *E. coli* crude extracts. Differences in the promoter region of *aidB* from those of *ada* and *alkA* could

explain the lower affinity of Ada for the promoter region of *aidB* and the necessity of an additional factor (Landini, Hajec et al. 1994).

AidB is known to be induced by *N*-methyl-*N'*-nitro-*N*-nitrosoguanidine (MNNG) and mutations in its gene affect sensitivity to MNNG but not to other alkylating agents (Volkert, Nguyen et al. 1986). Overexpression of *aidB* diminishes the mutagenic effects of MNNG (Landini, Hajec et al. 1994). Interestingly, some insertional mutants of *aidB* have the same phenotypic effect as its overexpression (Volkert, Nguyen et al. 1986). The reasons for this are unknown but it is possible that the mutants could produce a more a functional fragment of AidB with greater stability or activity than the wild-type protein (Landini, Hajec et al. 1994).

AidB binds double stranded (ds) DNA protecting the DNA from chemical modification (Rohankhedkar, Mulrooney et al. 2006). Through homology modeling it was found to be a tetramer with a positively charged groove conserved across AidB homologues. DNA binding to the groove arranges itself close to the active site of the enzyme (Rohankhedkar, Mulrooney et al. 2006). In addition there is a second larger groove in the fourth domain of AidB, which is less conserved, but likely also binds dsDNA. At this DNA binding site the stiff dsDNA is unable to interact with the active site, but it possibly serves a structural role. Homologues of the full-length *E. coli* AidB have not been found in some closely related bacteria including *Vibrio* and *Klebsiella* species. AlkA and AlkB homologues are found in most bacteria, suggesting that AidB may not be of primary importance for the adaptive response (Rohankhedkar, Mulrooney et al. 2006).

Distinct from its main functional role, AidB has also been found to have relatively weak isovaleryl-CoA dehydrogenase activity (Rohankhedkar, Mulrooney et al. 2006). These enzymes are active during fermentation and anaerobic metabolism for the production of energy (Brockman and Wood 1975). As cells shift into anaerobiosis AidB is expressed, which could explain a role for AidB as an acyl-CoA dehydrogenase (Landini, Hajec et al. 1994). Due to its enzymatically active flavin and DNA binding it was originally suggested that AidB directly repairs damaged DNA with a dehydrogenase activity (Rohankhedkar, Mulrooney et al. 2006). More recently is has been suggested that AidB protects DNA from alkylation damage through direct binding and protection against alkylating agents (Bowles, Metz et al. 2008). There is no obvious connection between ACP and AidB, although the large positively-charged DNA-binding groove in the latter could feasibly provide a site of interaction for the acidic ACP (Figure 8).

H. Objective and Thesis Rationale

The growth-dependent interaction of AidB and SpoT with ACP are both interesting, as neither of them appear to have an obvious direct involvement in lipid metabolism. However, as both of these proteins are involved in environmental stress responses, i.e. the stringent response for SpoT and the adaptive response for AidB, ACP could be relaying information about the metabolic state of the cell in attempts to coordinate lipid metabolism with responses to environmental stress. Based on the results of my Honours project, the objective of this project was to further characterize the SpoT-

24
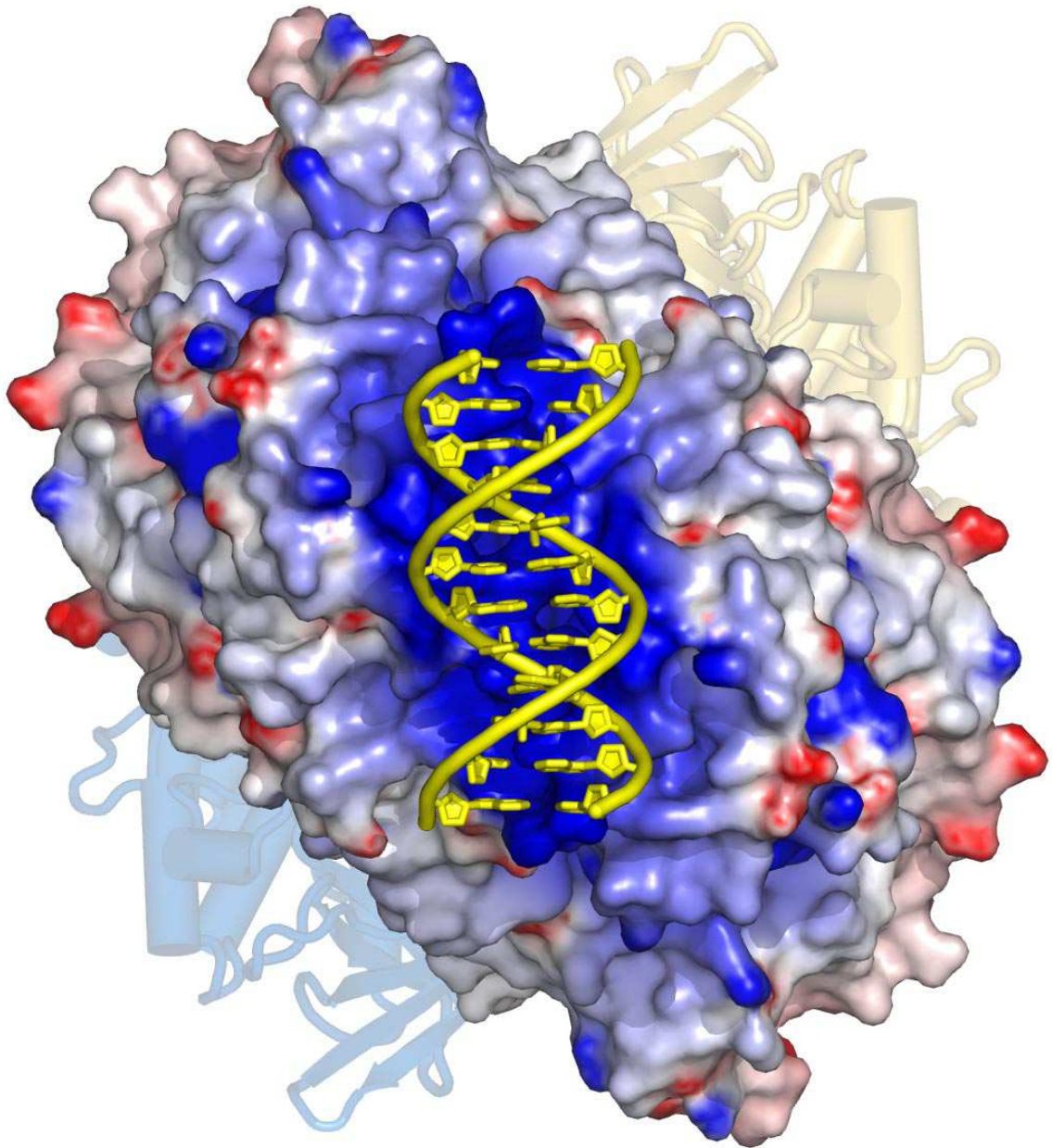
Figure 8: Model of the C-terminal DNA binding region of AidB. The blue and red
colouring represents basic and acidic regions of AidB. The dsDNA (yellow) is docked on
a basic AidB DNA binding site (adapted from Bowles et al. 2008).

ACP and AidB-ACP interactions, specifically to identify the regions and residues of ACP involved. The ultimate goal of this research is to enhance our knowledge of ACP interactions with partner enzymes, to aid in our understanding of the complete physiological role of ACP, and to provide insight into novel antibacterial strategies.

Chapter II: Materials and Methods

A. Materials

1. General Chemicals	Source
6x-His Monoclonal Antibody	ClonTech
30% Acrylamide/Bis Solution 37.5:1	Bio-Rad
AcTEV Protease	Invitrogen
Ampicillin, sodium salt	Sigma
Anti-FLAG M2 Agarose	Sigma
Anti-GST, HRP conjugated	Cell Signaling
Anti-Mouse IgG, HRP linked antibody (GAM)	Cell Signaling
Anti-Rabbit IgG, HRP linked antibody (GAR)	Cell Signaling
Anti-TAP Rabbit Polyclonal Antibody	Open Biosystems
BenchMark Prestained Protein Ladder	Invitrogen
Benzonase Nuclease, >99% purity	Novagen
Calmodulin Affinity Resin	Stratagene
GelCode Blue Stain	Pierce
Glutathione	Sigma
Glutathione sepharose 4B	Amersham Biosciences
His-SpinTrap, Ni^{2+} high performance columns	GE Healthcare
Iodoacetamide	Sigma
Isopropyl B-D-thiogalactopyranoside (IPTG)	Sigma-Aldrich

Kanamycin	Sigma-Aldrich
Luria-Bertani (LB) broth	EMD
pET23b(+) vector	Novagen
pGEX-5X-3 vector	GE Healthcare
PVDF Membrane	GE Healthcare
Rabbit IgG-agarose	Sigma
Restriction Enzymes and Buffers	New England Biolabs
Supersignal West Pico Chemiluminescent Substrate	Pierce
Surfact-Amps Triton X-100	Pierce
T4 DNA Ligase and Buffer	New England Biolabs
Tobacco Etch Virus (TEV) Protease	Invitrogen
Trypsin, Sequencing Grade Modified	Promega

2. Bacterial Strains

E. coli BL21 (DE3) - *F⁻ ompT gal dcm lon hsdS$_B$ (r$_B$⁻ m$_B$⁻) λ(DE3 [lacI lacUV5-T7 gene 1 ind1 sam7 nin5])*	Novagen
E. coli DH5α - *(fhuA2 Δ(argF-lacZ)U169 phoA glnV44 Φ80 Δ(lacZ)M15 gyrA96 recA1 relA1 endA1 thi-1 hsdR17)*	New England Biolabs
E. coli DH5α ACP-TAP	Dr. Gareth Butland University of Toronto
E. coli DH5α Ada-SPA	Open Biosystems
E. coli DH5α AidB-SPA	Open Biosystems
E. coli DH5α AlkA-SPA	Open Biosystems
E. coli DH5α AlkB-SPA	Open Biosystems

E. coli DH5α SpoT-TAP

Open Biosystems

3. Bacterial Growth Media

Luria Bertani (LB) broth

10 g NaCl, 10 g Bacto tryptone, 5 g yeast per L of H_2O

Solid medium

LB broth containing 16 g agar per L

Terrific Broth (TB)

12 g tryptone, 23.6 g yeast extract, 9.4 g K_2HPO_4, 2.2 g KH_2PO_4 per L of H_2O

4. Solutions

6x DNA loading buffer

0.25 % bromophenol blue, 0.25 % xylene cyanol FF, 30 % glycerol in water

SDS-PAGE sample buffer (4X)

125 mM Tris Base, 5% SDS, 25% glycerol, 0.25% bromophenol blue

SDS-PAGE sample buffer (1X)

4X SDS-PAGE sample buffer diluted with dH_2O 3:1

SDS-PAGE running buffer (10X)

25 mM Tris Base. 192 mM glycine, 1 % SDS

1X TAE

2.0 of Tris Base, 57.1 mL of acetic acid, 0.05 M EDTA, pH 8.0

TBS buffer

20 mM Tris Base, 0.1 M NaCl

1X TTBS

TBS containing 0.2 % Tween 20 (v/v)

1X PBS	137 mM NaCl, 2.7 mM KCl, 4.3 mM Na$_2$HPO$_4$, 1.47 mM KH$_2$PO$_4$, pH 7.4
PBST	PBS containing 0.4 % Tween 20 (v/v)

B. Methods

1. General Methods

i. Sodium Dodecyl Sulfate Polyacrylamide Gel Electrophoresis (SDS-Page)

Protein samples were resuspended in 1X SDS-PAGE sample buffer and heated to 95°C for 5 minutes. Samples were loaded onto a 1 mm thick SDS-polyacylamide gel alongside a BenchMark Prestained Protein Ladder and separated in 1X SDS running buffer at 150 V for 90 minutes using a Mini-PROTEAN II dual slab-cell (BioRad). Gels were washed in water three times for 5 minutes to remove excess SDS and stained with GelCode Blue reagent.

ii. Micro-Bicinchoninic Acid (Micro-BCA) Protein Assay

Protein concentrations were determined by comparison to bovine serum albumin (BSA) standards of 1 µg, 2 µg, 5 µg and 10 µg in 0.5 mL of distilled water. Two, 5, 10 and 20 µL aliquots of purified enzymes were diluted in 0.5 mL of distilled water. Micro BCA solution was prepared containing 50% Solution A, 48% Solution B, and 2% Solution C according to manufacturer's instructions (Pierce). Micro BCA solution (500 µL) was added to each of the samples. The samples were incubated for 60 minutes in a 60°C water bath, and then cooled to room temperature quickly with cold water. A standard curve was generated using the BSA standards with the absorbance read at 562

nm using a DU-640 spectrophotometer (Beckman Coulter). The concentrations of purified proteins were determined from the standard curve.

iii. Western Blotting

Proteins were transferred onto PVDF membranes from SDS-PAGE gels at 75 V for 2 hours. The membranes were dried overnight and incubated at room temperature with the primary antibody (anti-TAP (1:2000), anti-His6x (1:5000), or anti-GST conjugated with horseradish peroxidase (1:5000)) for one hour in 10 mL of 5% skim milk 1 X TTBS. The membranes were washed three times with 1X TBS for five minutes each and incubated with a secondary antibody conjugated with horseradish peroxidase if required (goat-anti-mouse diluted 1:5000, goat-anti-rabbit diluted 1:5000), for 30 minutes in 10 mL of 5% skim milk 1X TTBS. The membranes were washed six times with 1X TBS for five minutes each. Proteins were detected using SuperSignal West Pico Chemiluminescent Substrate (Thermo Scientific) and membranes were exposed to X-Omat Blue film (Kodak).

iv. Preparation of Chemically Competent *E. coli*

Each *E .coli* strain of interest was inoculated into 5 mL of TB broth at 30˚C with shaking at 200 rpm and grown overnight. Cells were then subcultured into 0.5 L of TB at 30˚C with shaking at 200 rpm until A_{600} measured 0.6. Cells were harvested by centrifugation at 5 000 rpm for 10 minutes at 4˚C. The remainder of the protocol was

performed in a cold room at 4°C. Cell pellets were resuspended in 167 mL of ice cold 0.1 M calcium chloride and incubated for four hours on ice. The samples were centrifuged at 5 000 rpm for 10 minutes. The pellets were resuspended in 16.7 mL of ice cold 0.1 M calcium chloride/15 % glycerol and incubated overnight. The samples were aliquoted into 100 µL and stored at -80°C.

v. *E. coli* Transformation.

E. coli cells containing the selected plasmid were cultured overnight in 2 mL LB broth at 30°C with shaking at 200 rpm. Cells were harvested by centrifugation at 7 500 x *g* for 3 min at room temperature. Plasmids were transformed into chemically competent cells by incubating 2.5 µL of selected plasmids and 100 µL of chemically competent cells on ice for 30 minutes, 42°C for 45 seconds, on ice for 2 minutes and then combined with 2.5 mL of SOC media for one hour at 37 °C. The samples were plated on LB plates with the required antibiotics for strain and plasmid selection (15 µg/µL kanamycin and/or 100 µg/µL ampicillin) and grown overnight at 37°C in a warm air incubator.

vi. Plasmid Isolation

From 5 mL *E. coli* cultures plasmids were isolated by mini-prep using Qia-spin columns as per manufacturer's instructions (Qiagen).

vii. DNA Agarose Gel Electrophoresis

DNA samples and a 1 kb DNA ladder standard (Invitrogen) were added to 6X
DNA loading buffer. Samples were loaded on a 1 % agarose gel with 0.5 µg/mL ethidium
bromide and separated in 1X TAE buffer at 100 V for 45 minutes using a Mini-Sub Cell
GT (BioRad) electrophoresis apparatus. Gel bands were visualized with UV light. DNA
was eluted from agarose gels using the Gene Clean kit (Qiagen) to remove agarose into 5
µL sterile water.

2. Protein Preparation

i. Purification of TAP and SPA Tagged Proteins

E. coli DH5α encoding genomic ACP-TAP or SpoT-TAP were inoculated into 5
mL of TB broth containing 15 µg/mL kanamycin at 30˚C with shaking at 200 rpm and
grown overnight. Cells were then subcultured into 0.5 L of TB broth containing 15
µg/mL kanamycin at 30˚C with shaking at 200 rpm until the optical density at 600 nm
(OD_{600}) measured 1.0. Cells were harvested by centrifugation at 7 500 x *g* for 15 min at
4˚C. The cell pellet was resuspended in 15 mL of cold lysis buffer (10 mM Tris-HCl, pH
8.0, 150 mM NaCl, 0.1% Triton X-100, 0.2 mM EDTA, 10% (v/v) glycerol, 0.5 mM
DTT) and 25 U of Benzonase nuclease (Novagen 70664-3), incubated on ice for 20
minutes, and lysed by sonication, 8 bursts of 30 seconds, using a probe sonicator. Cell

lysates were clarified by centrifugation at 20 000 x g for 30 minutes at 4˚C. The supernatant was added to IPP150 (10 mM Tris-HCl, pH 8.0, 150 mM NaCl, 0.1% Triton X-100, 10% (v/v) glycerol) equilibrated IgG agarose beads (100 µL packed volume) and incubated overnight at 4˚C, rotating end-over-end. Samples were applied to Poly-Prep chromatography columns (Bio-Rad) and washed with 30 mL of IPP150 buffer followed by 10 mL of TEV cleavage buffer (10 mM Tris-HCl, pH 8.0, 150 mM NaCl, 0.1% Triton X-100, 0.5 M EDTA, 10% (v/v) glycerol, 1 mM DTT). TEV cleavage buffer (1 mL) was added to the closed column with 100 Units of TEV protease (Gibco BRL). Sample was incubated for two hours at room temperature, rotating end-over-end. Column was drained by gravity, and an additional 200 µL of TEV cleavage buffer was washed through the column. The recovered sample was added to 3 mL of calmodulin binding buffer (10 mM Tris-HCl, pH 8.0, 150 mM NaCl, 0.1% Triton X-100, 1 mM Mg-acetate, 1 mM imidazole, 10% (v/v) glycerol, 2 mM $CaCl_2$, 10 mM β-mercaptoethanol) plus 3 µL of 1 M $CaCl_2$, and incubated for 1 hour at 4˚C rotating end-over-end. The column was drained by gravity and washed with 30 mL of calmodulin binding buffer. Bound proteins were eluted with 600 µL of calmodulin elution buffer (10 mM Tris-HCl, pH 8.0, 150 mM NaCl, 0.1% Triton X-100, 1 mM Mg-acetate, 1 mM imidazole, 5 mM EGTA, 2.5% (v/v) glycerol, 10 mM β-mercaptoethanol). The eluate was divided into two samples of 300 µL and precipitated with 1.5 mL of cold acetone stored overnight at -20˚C.

SPA tagged proteins, i.e. ACP-SPA, AidB-SPA, Ada-SPA, AlkA-SPA, and AlkB-SPA, were purified using the same method except for the first purification step. Instead of IgG agarose beads and washing with IPP150 buffer, anti-FLAG M2 agarose

was used and washing was performed with M2 buffer (10 mM Tris-HCl, pH 8.0, 100 mM NaCl, 0.1% Triton X-100, 10 % (v/v) glycerol).

ii. Cloning of AidB-His$_{6x}$

C-terminal tagged AidB-hexahistidine (His$_{6x}$) constructs were made using *E. coli* genomic DNA as a template for PCR amplification of the gene using primers 5'-TGA AAG CTT CAC ACA CAC TCC CCC-3' and 5'-CGA CAT ATG GTG CAC TGG CAA ACT C-3', TA-cloning into pCR2.1 Topo (Invitrogen), and subcloning using restriction enzymes HindIII and NdeI into the pET23b(+) (Novagen) bacterial expression vector. The resulting plasmid encoded the *aidB* open reading frame with the stop codon removed and an inserted His$_{6x}$ tag at the C-terminus. Plasmid inserts were sequenced by the DalGEN sequencing facility at Dalhousie University.

iii. Cloning of SpoT-His$_{6x}$

C-terminal tagged SpoT-hexahistidine (His$_{6x}$) constructs were made using *E. coli* genomic DNA as a template for PCR amplification of the gene using primers 5'-TGA AAG CTT ATT TCG GTT TCG GG -3' and 5'-CGA CAT ATG TTG TAT CTG TTT GAA AG -3', TA-cloning into pCR2.1 Topo (Invitrogen), and subcloning using restriction enzymes HindIII and NdeI into the pET23b(+) (Novagen) bacterial expression vector. The resulting plasmid encoded the *spoT* open reading frame with the stop codon

removed and an inserted His_{6x} tag at the C-terminus. Plasmids generated were sequenced by the DalGEN sequencing facility at Dalhousie University.

iv. Expression and Purification of AidB-His_{6x} and SpoT-His_{6x}

His_{6x} tagged proteins were purified subsequent to transformation of plasmids in the pET23b(+) vector into *E. coli* BL21(DE3). Cells were grown overnight in 2 mL of LB broth containing 100 µg/mL ampicillin at 30˚C shaking at 200 rpm. The cells were subcultured into 10 mL of LB broth containing 100 µg/mL of ampicillin at 30˚C with shaking at 200 rpm until the OD_{600} measured 0.5. Protein synthesis from the plasmid borne open reading frame was induced by the addition of IPTG to a final concentration of 0.2 mM with incubation for 3 hours at 30˚C. The cell cultures were dispensed into 2 mL aliquots and concentrated by centrifugation at 7 500 x *g* for 15 minutes. Purification was completed by using His-SpinTrap Ni High performance columns (GE Healthcare) following manufacturer's instructions. Purified proteins were stored at -20˚C.

v. Purification of GST-ACP

V. harveyi ACP, and ACP mutants F50A and SA/SB in the pGEX-5X-3 expression vector (Gong, Murphy et al. 2007) were transformed into *E. coli* BL21(DE3) cells. Cells were grown overnight in 2 mL of LB broth containing 100 µg/mL of ampicillin at 30˚C with shaking at 200 rpm and subcultured into 100 mL of LB broth containing 100 µg/mL of ampicillin at 30˚C with shaking at 200 rpm until OD_{600}

measured 0.5. Protein synthesis from the plasmid borne open reading frame was induced

by the addition of IPTG to a final concentration of 0.2 mM and incubated for another 3

hours at 30˚C. The cell cultures were harvested by centrifugation at 7 500 x g for 15

minutes at 4˚C. Cell pellets were resuspended in 4 mL PBS and sonicated four times for

30 seconds each using a probe sonicator. Triton X-100 was added to give a final

concentration of ~1% and samples were incubated on ice for 30 minutes. The cell lysates

were clarified by centrifugation at 20 000 x g for 30 minutes at 4˚C. Pellets were

resuspended in 4 mL of PBS and combined with 1 mL of PBS equilibrated glutathione

Sepharose and incubated end-over-end for 30 minutes at room temperature. The sample

was poured into a poly-prep chromatography column and washed with 30 mL of PBS.

GST-tagged proteins were eluted using 2 mL of freshly made reduced 10 mM glutathione

in 50 mM Tris-HCl, pH8.0. Eluates were stored at -20˚C.

3. Protein Interaction Studies

i. Far Western

AidB-His$_{6x}$ interaction with various ACP mutants was examined by far western

blotting. Purified AidB-His$_{6x}$ (6 µL) was spotted on a PVDF membrane, alongside 2 µg

of BSA standard and AcpS-His$_{6x}$, and left to dry overnight. The PVDF membrane was

blocked with 5% skim milk in 1X PBST (PBST 10X – 4 mM KH$_2$PO$_4$, 16 mM Na$_2$HPO$_4$,

115 mM NaCl, pH 7.4, 0.05 % Tween 20) for one hour. The PVDF membrane was

incubated overnight with GST-ACP or the control, GST, at a concentration of 1 µg/mL in

freshly prepared protein binding buffer (100 mM NaCl, 20 mM Tris, pH 7.6, 0.5 mM EDTA, 10 % glycerol, 0.1 % Tween 20, 2 % skim milk, 1 mM DTT) at 4˚C. To see if the GST-ACP bound the spotted AidB-His$_{6x}$, an anti-GST western blot was performed as follows. The PVDF membrane was washed with 1X PBST three times for 10 minutes at room temperature and incubated with anti-GST conjugated with HRP antibody at a 1:5 000 dilution for one hour at room temp in 5 % skim milk in 1X PBST. The membrane was washed five times for 10 min at room temperature in 5 % skim milk in 1X PBST. The membrane was washed five times for 10 minutes with 1X PBST and rinsed with PBS for 5 minutes. Proteins were detected by adding using SuperSignal West Pico Chemoluminescent Substrate to the membranes, and exposing the membranes to X-Omat Blue film (Kodak).

In order to estimate the relative amounts of AidB-His$_{6x}$ and AcpS-His$_{6x}$ bound to the PVDF membrane, an anti-His$_{6x}$ western blot was performed as described earlier in section 1. General Methods, on the original spotted PDVF membrane.

ii. GST-Pull Downs in SpoT-TAP Strains

Induction of GST, GST-ACP, and various GST-ACP mutants in the SpoT-TAP strain was performed for analysis of their binding to SpoT-TAP by GST pull down. DH5α (SpoT-TAP) cultures transformed with an empty pGEX vector, pGEX ACP or pGEX containing various ACP mutants were grown overnight in 2 mL of TB broth with 15 µg/mL kanamycin and 100 µg/mL ampicillin at 30˚C with shaking at 200 rpm. Cells were subcultured into 50 mL of TB broth containing 15 µg/mL kanamycin and 100

µg/mL ampicillin at 30˚C with shaking at 200 rpm until OD_{600} measured 0.5 at which 0.2

mM IPTG was added and cultures were incubated for another 2 hours at 30˚C with

shaking at 200 rpm. Cells were harvested by centrifugation at 7 500 x g for 15 minutes at

4°C. Cell pellets were resuspended in 2.5 mL of lysis buffer (10 mM Tris-HCl, pH 8.0,

150 mM NaCl, 0.1% Triton X-100, 0.2 mM EDTA, 10% (v/v) glycerol, 0.5 mM DTT)

and 1 µL of Benzonase nuclease, incubated on ice for 20 minutes, and sonicated with a

probe sonicator four times for 15 seconds. Cell lysates were clarified by centrifugation at

20 000 x g for 30 minutes at 4˚C. The supernatants were added to 250 µL of glutathione

Sepharose in a Poly-Prep chromatography column (Bio-Rad) and incubated end-over-end

for one hour at 4˚C. Columns were washed three times with 1 mL of lysis buffer using

gravity flow and protein eluted with lysis buffer containing 10 mM glutathione. Eluates

were stored at - 20˚C.

iii. Preparation of Samples for IDA and MRM Analysis

For MRM the acetone precipitates of the TAP and SPA elutions, and standards

(0.3 µg of bovine serum albumin (BSA), ovalbumin (OVA), cytochrome c (CytC), and

ACP) were made up to 30 µL with fresh 100 mM ammonium bicarbonate. Samples were

reduced by the addition of 200 mM DTT to a final concentration of 5 mM and incubated

at 60˚C for 30 min. Samples were then treated with 200 mM iodoacetamide to give a

final concentration of 15 mM and incubated in the dark at room temperature for 30 min.

The samples were then made up to a final volume of 300 µL in 100 mM ammonium

bicarbonate. Sequencing grade trypsin was prepared by diluting the 20 µg stock with 200

μL of 50 mM acetic acid to give 0.1 µg/µL concentration of trypsin. The samples were digested with 1 µL of trypsin by incubation for 20 hrs at 37˚C in a warm air incubator. The digested samples were diluted 2 fold with 10% acetonitrile, 0.5 % formic acid and 6 µL was injected into a mass spectrometer for analysis.

HPLC/MS/MS was performed using an Ultimate pump and Famos auto-sampler (LC Packings, Amsterdam, Netherlands) interfaced to the nanoflow ESI source of a hybrid triple quadrupole linear ion trap (*Qtrap*) mass spectrometer (Applied Biosystems, Foster City, CA, USA). Data were searched using the MASCOT (version 1.6b21) algorithm against the NCBI non-redundant protein database (20080924) using MS/MS ion searching. For experiments one and two the transitions scanned for are in Tables 2 and 3, respectively. See Table 4 for description of peptides searched for in experiment 3.

Peptide		Q1 mass (mass of peptide)	Q2 mass (mass of fragment)	Collision energy	Dwell time (s)
ACP	IIGEQLGVK	478.8	730.4	24	60
		478.8	843.5	24	60
		478.8	199.2	24	60
SPOT	SVAELVEGVSK	559.3	931.7	27	60
		559.3	618.5	27	60
		559.3	159.1	27	60
	TELEELGFEALYPNR	890.9	1066.4	42	60
		890.9	386.3	42	60
		890.9	862.7	42	60
	SDLFPDEIYVFTPEGR	942	1423.1	44	60
		942	458.4	44	60
		942	805.7	44	60
AIDB	LANVNPPELLR	618.4	627.4	30	60
		618.4	1051.6	30	60
	FLPDGQR	416.7	572.3	21	60
		416.7	512.3	21	60
ALKB	FAFNAAEQLIR	640.3	800.4	31	60
		640.3	729.4	31	60
		640.3	219.1	31	60
	DINDVASQSPFR	674.8	419.2	32	60
		674.8	891.5	32	60
ALKA	GVVTAIPDIAR	556.3	571.3	27	60
		556.3	524.3	27	60
	LAAADPQALK	499.3	556.3	25	60
		499.3	442.2	25	60
ADA	GDGTLSGYR	463.2	696.4	23	60
		463.2	753.4	23	60
	DTPLTLPLDIR	627.4	613.4	30	60
		627.4	1037.6	30	60
		627.4	217.1	30	60

Table 2: Transitions used in MRM MS scans of ACP-TAP eluates: experiment 1. ACP, SpoT, and AidB transitions were acquired from previous results (from J. Cottle, Hons project). Transitions for Ada, AlkA, and AlkB were chosen based on properties that are important for identifying peptides through MS scans.

Peptide		Q1 mass (mass of peptide)	Q3 mass (mass of fragment)	Dwell time (s)	Collision energy
SpoT	SVAELVEGVSK	559.3	931.7	60	27
		559.3	618.5	60	27
		559.3	159.1	60	27
	TELEELGFEALYPNR	890.9	1066.4	60	42
		890.9	386.3	60	42
		890.9	862.7	60	42
AidB	LANVNPPELLR	618.4	627.4	60	30
		618.4	1051.6	60	30
	LSEQIQNDLLLR	721.4	871.5	60	28
		721.4	984.6	60	28
		721.4	458.2	60	28
	M_{ox}ALQLEGQTALLFR	803.9	332.2	60	32
		803.9	1034.6	60	32
		803.9	1147.6	60	32
	QAGVYDLLSEAFVEVK	590	692.4	60	21
		590	908.5	60	21
		884.4	908.5	60	36
		884.4	1021.6	60	36
AlkB	FAFNAAEQLIR	640.3	800.4	60	31
		640.3	729.4	60	31
		640.3	219.1	60	31
Keratin		651.8	1102.6	60	32
		651.8	987.6	60	32

Table 3: Transitions used in MRM MS scans of ACP-TAP eluates: experiment 2. SpoT, AidB, and keratin transitions were acquired from previous results (from J. Cottle, Hons project) and used as controls. Transitions for Ada, AlkA, and AlkB were chosen based on properties that are important for identifying peptides through MS scans

Peptide		Q1 mass (mass of peptide)	Q3 mass (mass of fragment)	Dwell time (s)	Collision energy
Ada	GDGTLSGYR	463.2	868.4	60	23
		463.2	753.4	60	23
		463.2	696.4	60	23
		463.2	595.3	60	23
		463.2	482.2	60	23
		463.2	395.2	60	23
		463.2	338.2	60	23
		463.2	173.1	60	23
		463.2	145.1	60	23
	AVASACAANK	481.7	891.4	60	24
		481.7	792.4	60	24
		481.7	721.3	60	24
		481.7	634.3	60	24
		481.7	563.3	60	24
		481.7	403.2	60	24
		481.7	332.2	60	24
		481.7	171.1	60	24
		481.7	143.1	60	24
	YALADCELGR	584.3	1004.5	60	29
		584.3	933.4	60	29
		584.3	820.4	60	29
		584.3	749.3	60	29
		584.3	634.3	60	29
		584.3	474.3	60	29
		584.3	345.2	60	29
		584.3	235.1	60	29
		584.3	207.1	60	29
	DPNADGEFVFAVR	718.8	1321.7	60	35
		718.8	1224.6	60	35
		718.8	1110.6	60	35
		718.8	1039.5	60	35
		718.8	924.5	60	35
		718.8	867.5	60	35
		718.8	738.4	60	35
		718.8	213.1	60	35
		718.8	185.1	60	35
	DTPLTLPLDIR	627.4	1037.6	60	31
		627.4	940.6	60	31
		627.4	827.5	60	31
		627.4	726.5	60	31
		627.4	613.4	60	31

Peptide		Q1 mass (mass of peptide)	Q3 mass (mass of fragment)	Dwell time (s)	Collision energy
Ada	DTPLTLPLDIR	627.4	516.3	60	31
		627.4	403.2	60	31
		627.4	217.1	60	31
		627.4	189.1	60	31
	EVIASLNQR	515.3	900.5	60	26
		515.3	801.5	60	26
		515.3	688.4	60	26
		515.3	617.3	60	26
		515.3	530.3	60	26
		515.3	417.2	60	26
		515.3	303.2	60	26
		515.3	229.1	60	26
		515.3	201.1	60	26
	ATCLTDDQR	540.2	1008.4	60	27
		540.2	907.4	60	27
		540.2	747.4	60	27
		540.2	634.3	60	27
		540.2	533.2	60	27
		540.2	418.2	60	27
		540.2	303.2	60	27
		540.2	173.1	60	27
		540.2	145.1	60	27
AlkA	SLAVGEYR	447.7	807.4	60	23
		447.7	694.4	60	23
		447.7	623.3	60	23
		447.7	524.2	60	23
		447.7	467.2	60	23
		447.7	201.1	60	23
		447.7	173.1	60	23
	LPGCVDAFEQGVR	724.3	1020.5	60	35
		724.3	921.4	60	35
		724.3	806.4	60	35
		724.3	735.4	60	35
		724.3	588.3	60	35
		724.3	459.3	60	35
		724.3	331.2	60	35
		724.3	211.1	60	35
		724.3	183.1	60	35
	TLQTFPGIGR	545.3	988.6	60	27
		545.3	875.5	60	27
		545.3	747.4	60	27
		545.3	646.4	60	27

Peptide		Q1 mass (mass of peptide)	Q3 mass (mass of fragment)	Dwell time (s)	Collision energy
AlkA	TLQTFPGIGR	545.3	499.3	60	27
		545.3	402.2	60	27
		545.3	345.2	60	27
		545.3	215.1	60	27
		545.3	187.1	60	27
	WTANYFALR	571.3	1141.6	60	28
		571.3	955.5	60	28
		571.3	854.5	60	28
		571.3	783.4	60	28
		571.3	669.4	60	28
		571.3	506.3	60	28
		571.3	359.2	60	28
		571.3	288.1	60	28
		571.3	260.1	60	28
	AILGQLVSVAMAAK	686.4	1017.6	60	33
		686.4	889.5	60	33
		686.4	776.4	60	33
		686.4	677.4	60	33
		686.4	590.3	60	33
		686.4	491.3	60	33
		686.4	420.2	60	33
		686.4	185.1	60	33
		686.4	157.1	60	33
	LAAADPQALK	499.3	884.5	60	25
		499.3	813.4	60	25
		499.3	742.4	60	25
		499.3	671.4	60	25
		499.3	556.3	60	25
		499.3	459.3	60	25
		499.3	331.2	60	25
		499.3	185.1	60	25
		499.3	157.1	60	25
	VAQLYER	468.2	836.4	60	24
		468.2	765.4	60	24
		468.2	637.3	60	24
		468.2	524.2	60	24
		468.2	361.2	60	24
		468.2	304.2	60	24
		468.2	171.1	60	24
		468.2	143.1	60	24
AlkB	DINDVASQSPFR	674.8	1006.5	60	33
		674.8	891.5	60	33

Peptide		Q1 mass (mass of peptide)	Q3 mass (mass of fragment)	Dwell time (s)	Collision energy
AlkB	DINDVASQSPFR	674.8	792.4	60	33
		674.8	721.4	60	33
		674.8	634.3	60	33
		674.8	506.3	60	33
		674.8	419.2	60	33
		674.8	229.1	60	33
		674.8	201.1	60	33
	FAFNAAEQLIR	640.3	1061.6	60	31
		640.3	914.5	60	31
		640.3	800.5	60	31
		640.3	729.4	60	31
		640.3	658.4	60	31
		640.3	529.3	60	31
		640.3	401.3	60	31
		640.3	219.1	60	31
		640.3	191.1	60	31

Table 4: Transitions used in MRM MS scans of Ada, AlkA, and AlkB: experiment 3. These proteins were selected using Peptide Sieve software.

Chapter III. Results

A. Relative Expression of TAP And SPA Tagged Proteins

1. Relative Expression of ACP-TAP, SpoT-TAP, AidB-SPA as a Function of Growth Using Anti-TAP Antibodies

As described in the introduction, my Honours work found increased amounts of SpoT and AidB bound to ACP-TAP in late stationary phase compared to that bound at early stages of growth (Figure 7). To determine if the increase of SpoT and AidB bound to ACP in stationary phase was a result of increased gene expression or increase protein-protein affinity, we examined the levels of the individual proteins during log phase and stationary phase. All three strains, ACP-TAP, SpoT-TAP, and AidB-SPA in DH5α *E. coli* were grown to early log phase, late log phase, as well as stationary phase and cell extracts were prepared. The amount of sample separated on SDS-PAGE gels was corrected for cell (optical) density so as to normalize to the same number of cells across the different growth stages. Protein expression was visualized using anti-TAP western blots. Film exposures varied for each of the strains because of the dramatic variance of cellular amounts of the individual proteins. ACP-TAP was exposed for 30 seconds, SpoT-TAP was exposed for 10 minutes, while AidB-SPA was exposed overnight (Figure 9). From these results, it is clear that ACP-TAP and SpoT-TAP are constitutively expressed (panels a and b, respectively), while AidB-SPA is only expressed during stationary phase (panel c).
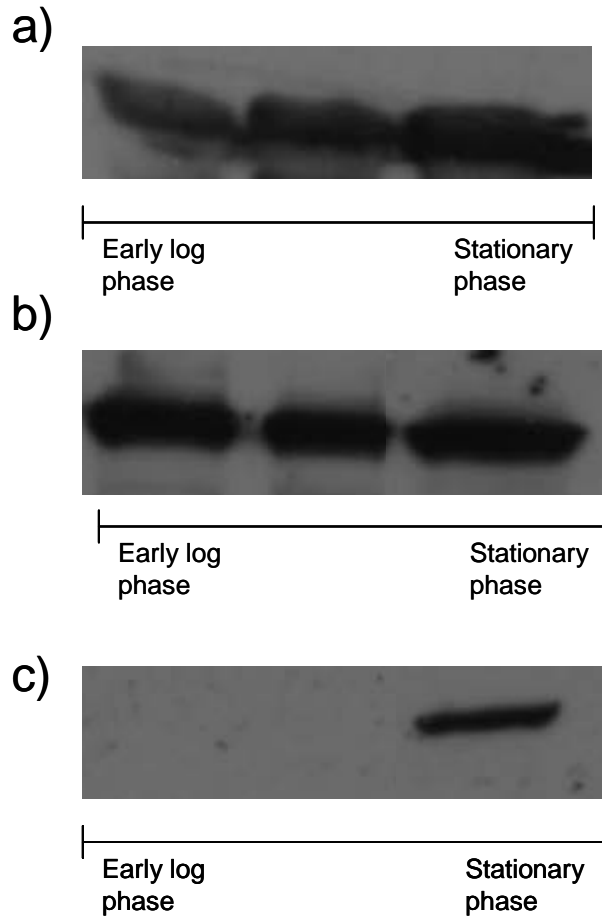
a)

Early log
phase

Stationary
phase

b)

Early log
phase

Stationary
phase

c)

Early log
phase

Stationary
phase

Figure 9: *E. coli* DH5α ACP-TAP, SpoT-TAP, and AidB-SPA visualized by anti-TAP western blot. Cell extracts were harvested during early log phase ($OD_{600} = 0.5$), late log phase ($OD_{600} = 1.0$), and stationary phase ($OD_{600} = 2.0$). Blots for each cell type had to be exposed for different times for visualization. ACP-TAP (a) was exposed for 30 seconds, SpoT-TAP (b) was exposed for 10 minutes, and AidB-SPA (c) was exposed overnight.

Determination of the levels of the three other adaptive response proteins, Ada-SPA, AlkA-SPA, and AlkB-SPA, in DH5α *E. coli* was also attempted as a function of growth status, but these proteins could not be visualized by anti-TAP western blotting, possibly due to very low levels of expression at all growth states.

2. Anti-TAP Detection of TAP versus SPA Tagged Proteins

The anti-TAP antibody (Open Biosystems) is specific for the C-terminus of the TAP construct after TEV cleavage, i.e. the calmodulin binding peptide and the remaining residues from the TEV cleavage site. For both TAP and SPA tags these regions are the same (Figure 4). To ensure that the anti-TAP antibody was detecting both the SPA and the TAP tags with relatively similar sensitivity, ACP-TAP and ACP-SPA DH5α strain extracts were examined by anti-TAP western blotting (Figure 10). Both ACP-TAP and ACP-SPA were clearly identified by the anti-TAP antibody and at comparable levels, although increased sensitivity to the anti-SPA antibody was noted. Due to the large differences in expression among ACP-TAP, SpoT-TAP, and AidB-SPA, I was unable to perform relative quantification of these proteins.
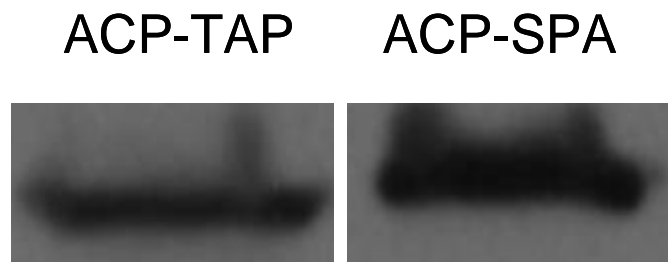
ACP-TAP   ACP-SPA

Figure 10: Anti-TAP western blot of ACP-TAP and ACP-SPA DH5α bacterial strains. Cell extracts of *E. coli* DH5α ACP-TAP and ACP-SPA strains were harvested at $OD_{600} =$ 0.7. Samples were separated by 15% SDS-PAGE and further analyzed by anti-TAP western blotting. Both were exposed for one minute.

B. Further Identification of ACP Bound Proteins by Mass Spectrometry

1. IDA Analysis of ACP-TAP In-Solution Digests

In initial attempts to identify ACP-TAP bound proteins present in low amounts we performed a tryptic digest of the entire affinity purified preparation for subsequent examination of the ACP-TAP eluates by information dependent acquisition (IDA) mass spectrometry. IDA is a "discovery" based approach that assumes no knowledge of the sample, but rather selects peptides for MS/MS fragmentation based on abundance as they elute during the LC gradient. Table 5 contains the proteins found during the MASCOT search of the results obtained from the MS/MS data. Although we identified a greater total number of proteins through excision and analysis of individual SDS-PAGE bands from the whole ACP-TAP purification elutes, the in-solution digest saves time and uses substantially less sample, allowing for further analysis of the purified preparation. The in-solution digest is also more sensitive, as seen with the identification of MukF, which was not visible on a SDS-PAGE gel. However, we did not observe other Ada response proteins that (like AidB) have DNA binding regions and might be expected to interact with ACP.

In-solution digest	
ACP-TAP co-purified proteins	Function
AcpP	acyl carrier protein
Aas	2-acylglycerophosphoethanolamine acyl transferase-acyl-acyl carrier protein synthetase: long chain fatty acid CoA ligase
AidB	isovaleryl-CoA dehydrogenase: in B-oxidation of fatty acids
FabB	3-oxoacyl-ACP synthase: involved in FAS II
FabF	3-oxoacyl-ACP synthase: involved in FAS II
FabG	3-oxoacyl-ACP reductase: involved in FAS II
IscS	cysteine desulfurase: alanine biosynthesis III
LpxD	UDP-3-O-(3-hydroxymyristoyl) glucosamine N-acyltransferase: involved in Lipid A synthesis
MukB	involved in chromosome partitioning
MukF	involved in chromosome partitioning
SpoT	guanosine-3',5'-bis(diphosphate) 3'-pyrophosphohydrolase: first step in ppGpp metabolism
YiiD	Acetyltransferase

Table 5: ACP-TAP binding proteins identified by IDA MS/MS after an in-solution digest of the whole eluate.

2. Multiple Reaction Monitoring (MRM) of ACP-TAP Digests for Ada, AlkA, and AlkB

Having demonstrated that proteins could be identified from the tryptic digest of affinity purified ACP-TAP eluates using IDA, we developed MRM protocols, initially looking for peptides known to be in the sample (i.e. from ACP, AidB, and SpoT). MRM repetitively searches for "prototypic" peptides (i.e. diagnostic for a specific protein) as they elute from the LC gradient; these are identified by "transitions", or fragmentation of a specific peptide precursor to specific products. A MRM scan is faster and much more sensitive than an IDA scan, as other molecules outside the narrow mass scan range do not reach the detector. However, MRM requires knowledge (or an educated guess) of which transitions will be observed. Ideally, these are selected with the knowledge gained from previous IDA MS/MS runs that identified peptides that were easily ionized as well as their major fragmentation products, e.g. as obtained during my honours work in 2007. Using this approach, we successfully identified all three control proteins, ACP, AidB, and SpoT (Figure 11 and Figure 12). Both MRM figures shown were scans of the same the ACP-TAP eluate tryptic digest, but in both scans we looked for different peptides and transitions. Not all peptides and transitions scanned for were found.

MRM MS scans were also extended to search for the three other adaptive response proteins, using peptides that we thought would be easily ionized and identified (Table 2 and Table 3). Initially, we selected these peptides based on characteristics common in peptides identified by MS, as we had no previous MS/MS data on these proteins, nor were we able to access this information from databases or the literature. Two transitions of one peptide for AlkA were seen over the two experiments and one
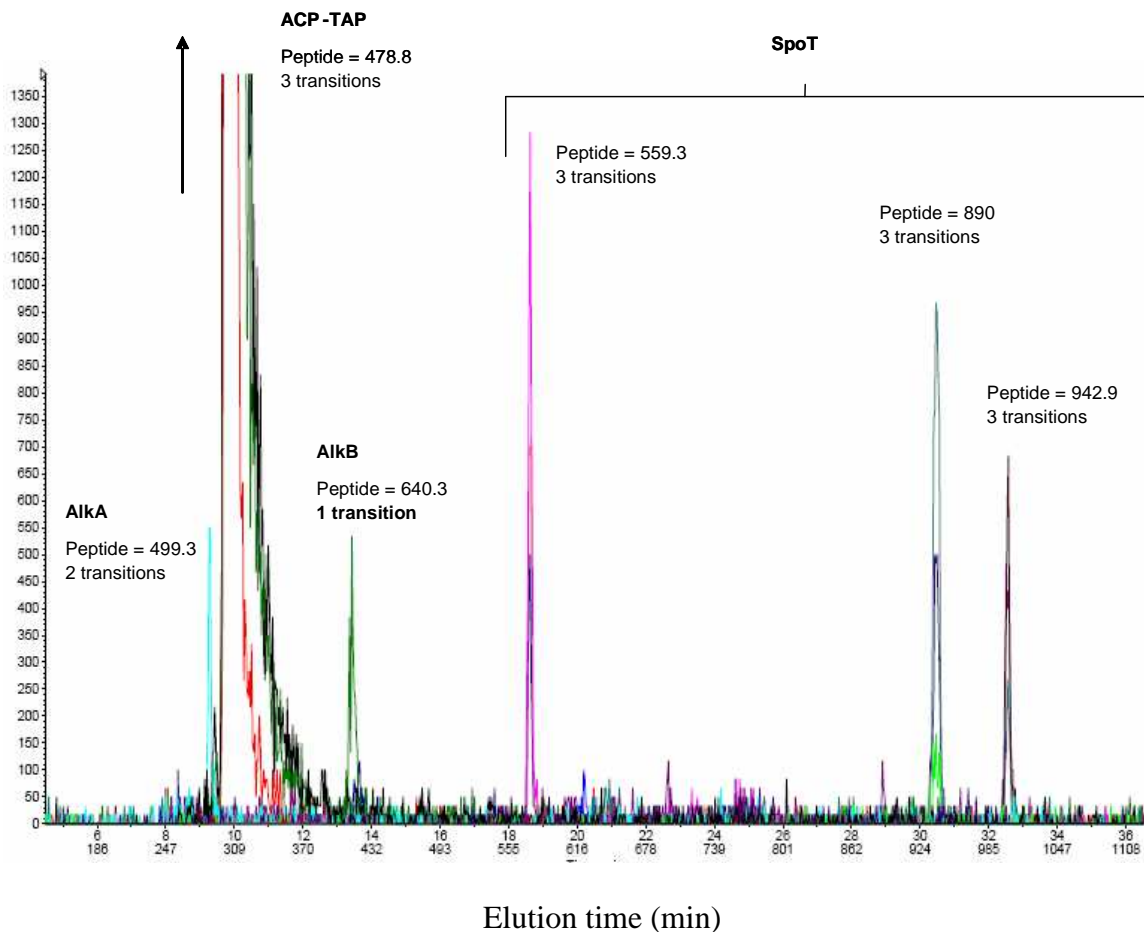
Figure 11: MRM analysis of an ACP-TAP eluate: experiment 1. The peptides and fragments listed in Table 2 were analyzed on the hybrid triple quadrupole linear ion trap (*Qtrap*) mass spectrometer (Applied Biosystems, Foster City, CA, USA). The peptides and the transitions identified are noted in different colours, where co-elution from the LC gradient of two or more transitions from a given peptide are indicative of its presence in the sample.
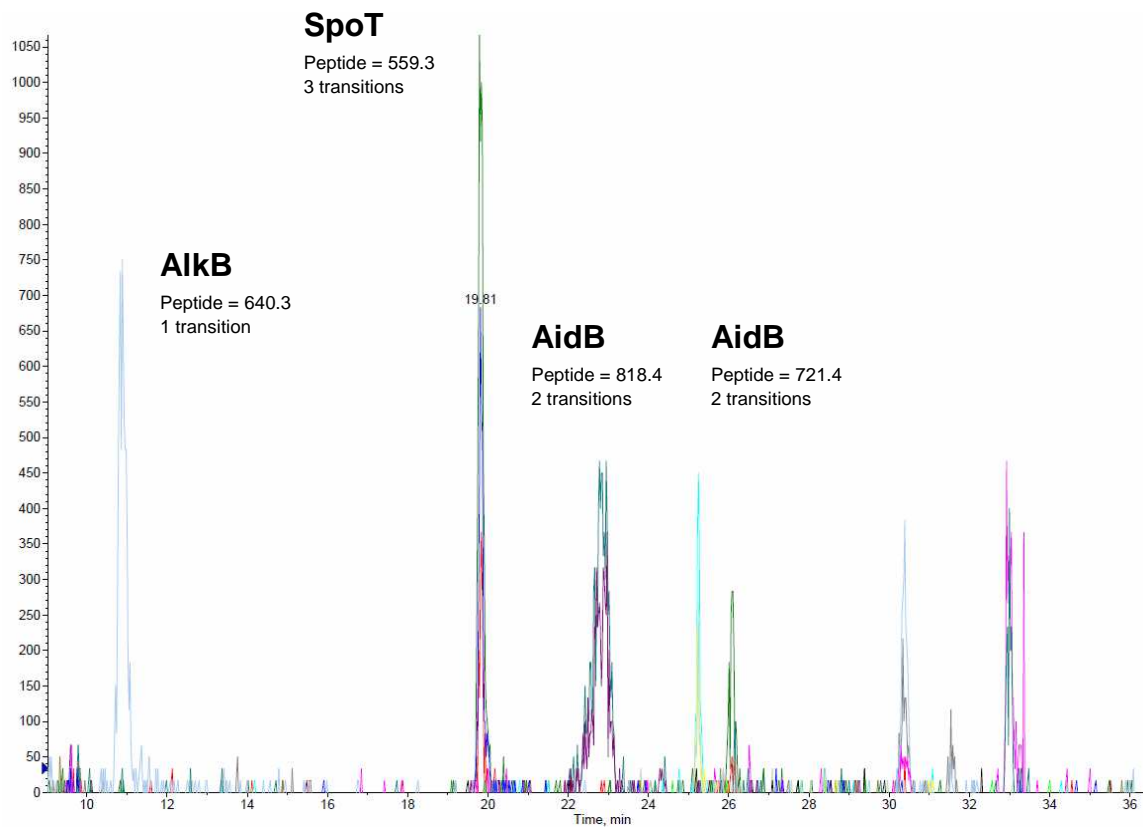
Figure 12: MRM analysis of an ACP-TAP eluate: experiment 2. The peptides and transitions listed in Table 3 were analyzed on a Qtrap hybrid triple quadrupole linear ion trap. Selected peptides and the transitions identified are noted.

transition of one peptide of AlkB was seen twice in two different MRM scans of an ACP-TAP eluate (Figure 11 and 12). The transitions of AlkA and AlkB in Figures 11 and 12 are of low mass, which suggests that these may be non-specific. Another experiment (Table 4), that was separated into three MRM MS scans gives the strongest evidence that AlkA may be present in the ACP-TAP eluate. The majority of the transitions identified were again of the lower fragment masses, againsuggesting non-specific transitions. The exception being the 545 massed peptide of AlkA, which had 8 of its 9 transitions identified. This is the most convincing result suggesting that AlkA may be in the ACP-TAP eluate and may be a possible binding partner of ACP, but this requires further verification.

3. MRM Analysis of Ada-SPA, AlkA-SPA, and AlkB-SPA Samples

As a complementary approach to the ACP-TAP purification experiemetns, we also examined affinity-purified material from Ada-SPA, AlkA-SPA, and AlkB-SPA expressing strains, both for the presence of these proteins and for any ACP that may have co-purified with them. Acetone precipitation of the SPA-tagged protein eluate was used to concentrate the samples prior to separation on an SDS-PAGE gel. As noted earlier, levels of Ada-SPA, AlkA-SPA, and AlkB-SPA were insufficient to visualize these proteins or any of their binding partners on the SDS-PAGE gels or by western blotting. We also prepared in-solution digests of the purified Ada-SPA, AlkA-SPA, and AlkB-SPA eluates for MRM analysis of potential ACP peptides, but unfortunately were unable to detect peptides from Ada, AlkA, or AlkB, or from any ACP that may have co-purified.

57

C.   Interaction Studies

1. Expression and Purification of AidB-His$_{6x}$ and SpoT-His$_{6x}$

An original goal of this project was to characterize the in vitro interactions between ACP and both SpoT and AidB, in particular to use our extensive ACP mutant collection to define the features of ACP required for binding. To this end, both AidB-His$_{6x}$ and SpoT-His$_{6x}$ were constructed in pET23b vectors and expressed in *E. coli* BL21 cells. Although both SpoT-His$_{6x}$ (Figure 13) and AidB-His$_{6x}$ (Figure 14) constructs of the expected size were expressed and could be enriched by Co^{2+} affinity chromatography, levels of both proteins were clearly insufficient to be visualized by protein staining, thus preventing use in standard binding assays with pure ACP. As a result, other methods of examining protein interactions were explored.

2. Examining Protein Interactions in vivo Using GST-ACP Expressed In SpoT-TAP or AidB-TAP Strains

As an alternate approach to examine ACP interactions with SpoT and AidB, we transformed the SpoT-TAP and AidB-SPA DH5α strains with a pGEX plasmid expressing GST-ACP fusion protein (Flaman et al 2001). As shown in Figure 15, GST-ACP expression was inducible with IPTG in the DH5α strain, although not to the extent observed in BL21 cells, as expected. Induction of either GST (empty pGEX vector) or

Elution of SpoT-HIS$_{6x}$

180 kD
115 kD
82 kD
64 kD
49 kD
37 kD
26 kD

Figure 13: Western blot of SpoT-His$_{6x}$ eluted from Co^{2+} affinity resin. After separation on a 15 % SDS-PAGE gel the protein was transferred to PVDF membrane. An anti-His$_{6x}$ western was used to visualize SpoT-His$_{6x}$. While a band was detected of the expected size (80 kDa), Coomassie or silver stained SDS-PAGE gel showed no protein bands.
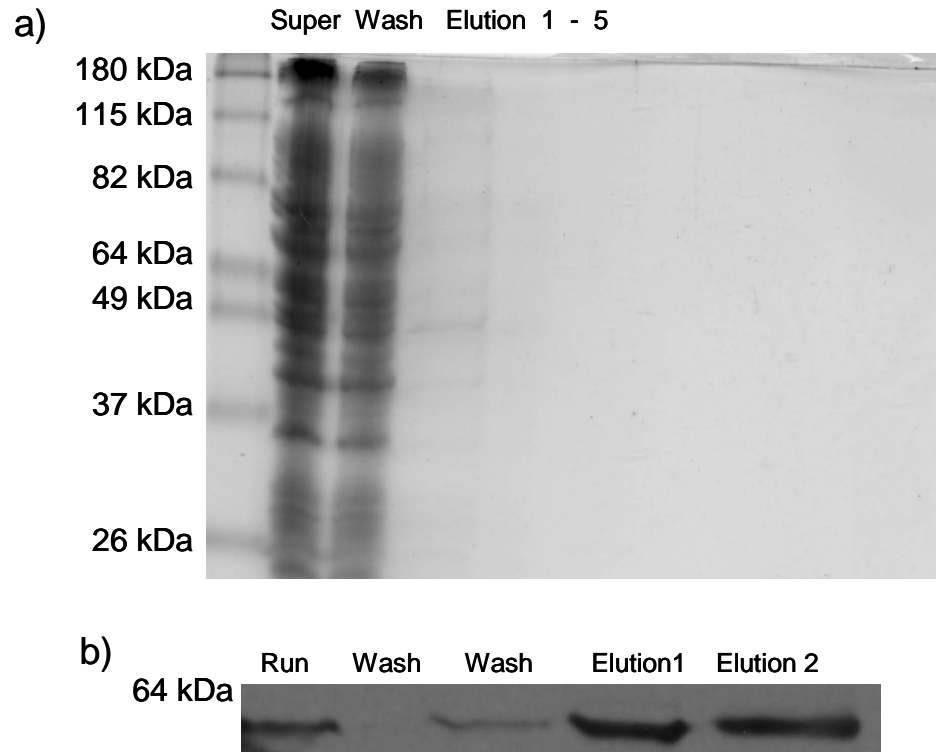
Figure 14: Expression and purification of AidB-His$_{6x}$. SDS-PAGE and anti-His$_{6x}$ Western blot of AidB-His$_{6x}$ purified by Co2+ affinity chromatography. Purified AidB-His$_{6x}$ could not be visualized by Gel-Code staining (a) but was visualized in an Anti-His$_{6x}$ western blot (b).

BL21 (DE3)   DH5a
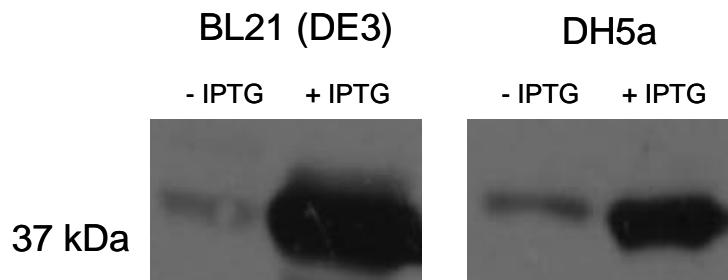
- IPTG   + IPTG   - IPTG   + IPTG

37 kDa

Figure 15: Anti-GST western blot of transformed *E. coli* BL21(DE3) and DH5α. Cells were transformed with a pGEX plasmid encoding GST-ACP. GST-ACP was induced with 0.2 mM IPTG in both BL21 and DH5α strains and separated on SDS-PAGE before visualization.

GST-ACP in SpoT-TAP DH5α cells had no effect on the constitutive level of SpoT expression, as indicated by an anti-TAP western blot (Figure 16, upper panel).

Once it was established that both the induced GST-ACP and the SpoT-TAP were expressed in these cells, glutathione-Sepharose chromatography was used to isolate the GST or GST-ACP, followed by SDS-PAGE and western blotting to determine if SpoT-TAP remained bound (Figure 17). Anti-TAP western blotting revealed that SpoT-TAP co-purified with GST-ACP but not with the control empty vector GST (Fig. 17, panel A). This experiment was repeated with GST fusion proteins of two ACP mutants, F50A (which is unable to fold properly) and SA/SB (in which the recognition helix II is neutralized) (Figure 18). The results clearly indicate that SpoT-TAP co-purifies with wild type GST-ACP but with neither of the mutants, suggesting that both the F50A and SA/SB mutants of ACP cannot bind SpoT.

A similar approach was attempted using the AidB-SPA DH5α strain. Although this strain was successfully transformed with the pGEX plasmids, it became apparent that when either GST or GST-ACP was induced with IPTG the levels of AidB in the cell was greatly decreased (Figure 19 and Figure 20). This effect seemed to be more dramatic for GST-ACP than for GST, although the extent of AidB decrease varied somewhat among different experiments. In any case, this suggests that either the degradation or synthesis of AidB is being affected during the IPTG induction process.
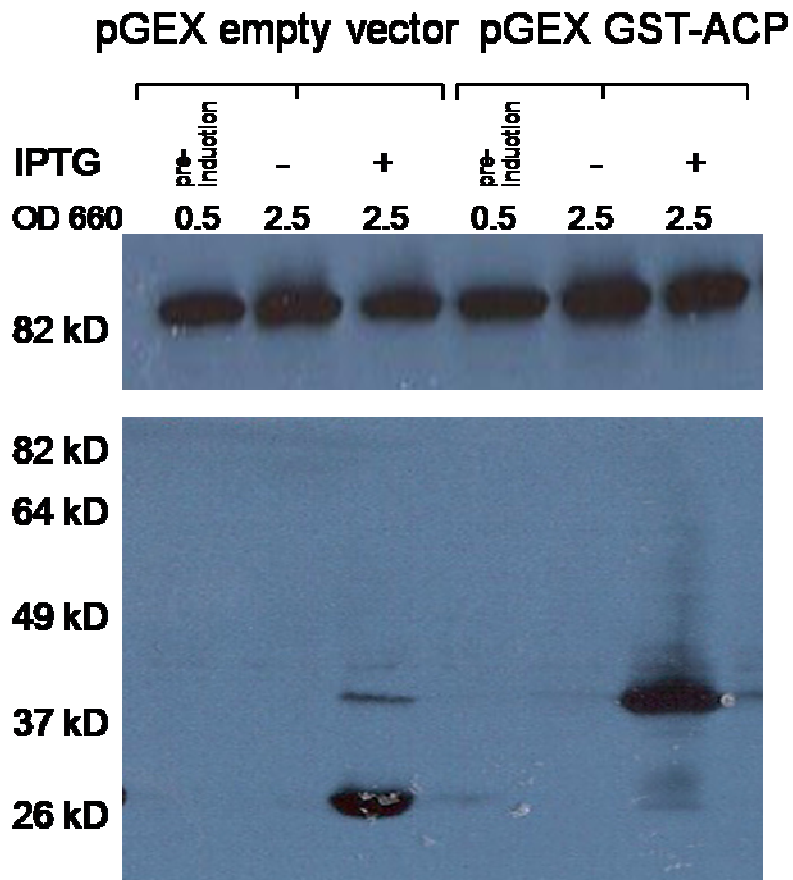
Figure 16: Western blot of induced GST-ACP in *E. coli* DH5α SpoT-TAP. SpoT-TAP was visualized with anti-TAP antibody (upper panel), while GST (approximately 26 kDa) and GST-ACP (approximately 40 kDa) were visualized with anti-GST antibody (lower panel).
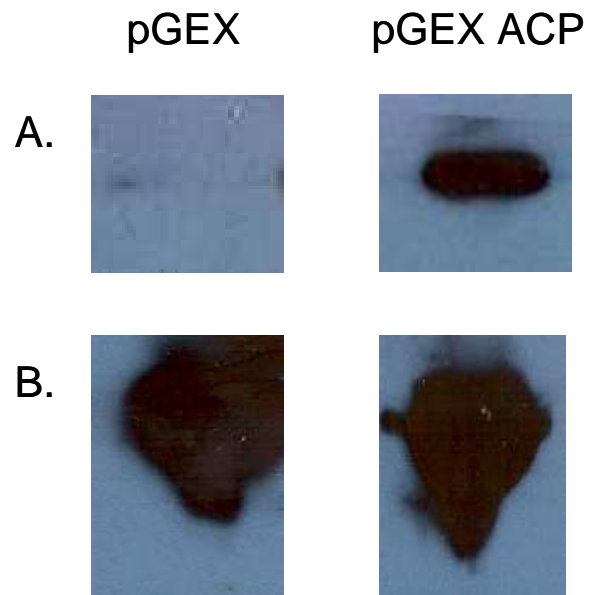
pGEX   pGEX ACP

A.

B.

Figure 17: Interaction of SpoT with GST-ACP but not GST. Following glutathione-Sepharose chromatography of extracts from *E. coli* DH5α SpoT-TAP cells expressing GST or GST-ACP, SpoT-TAP was identified with anti-TAP antibodies (A), while anti-GST was used to visualize the purified GST or GST-ACP (B).
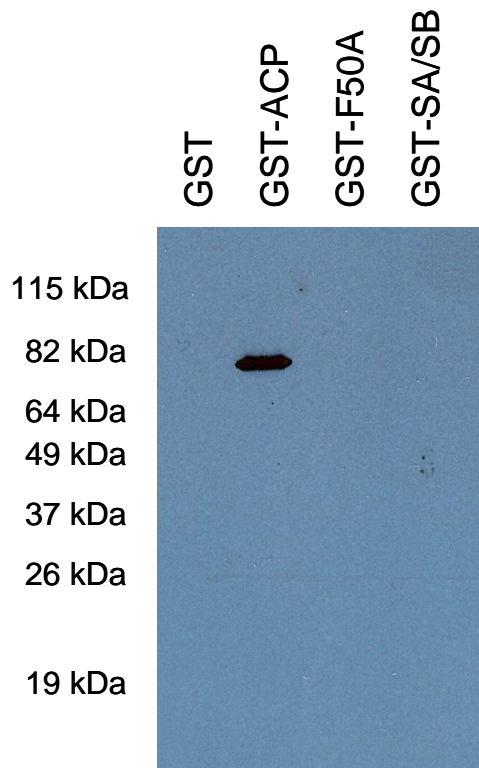
Figure 18: Specificity of SpoT-ACP interaction. SpoT-TAP strains transformed with empty vector pGEX (GST), pGEX-ACP (GST-ACP), pGEX-F50A (GST-F50A), or pGEX-SA/SB (GST-SA/SB) were induced with IPTG and cell extracts were subjected to glutathione-Sepharose chromatography. Anti-TAP western blotting was performed to see if SpoT-TAP co-purified with any of the induced ACPs.
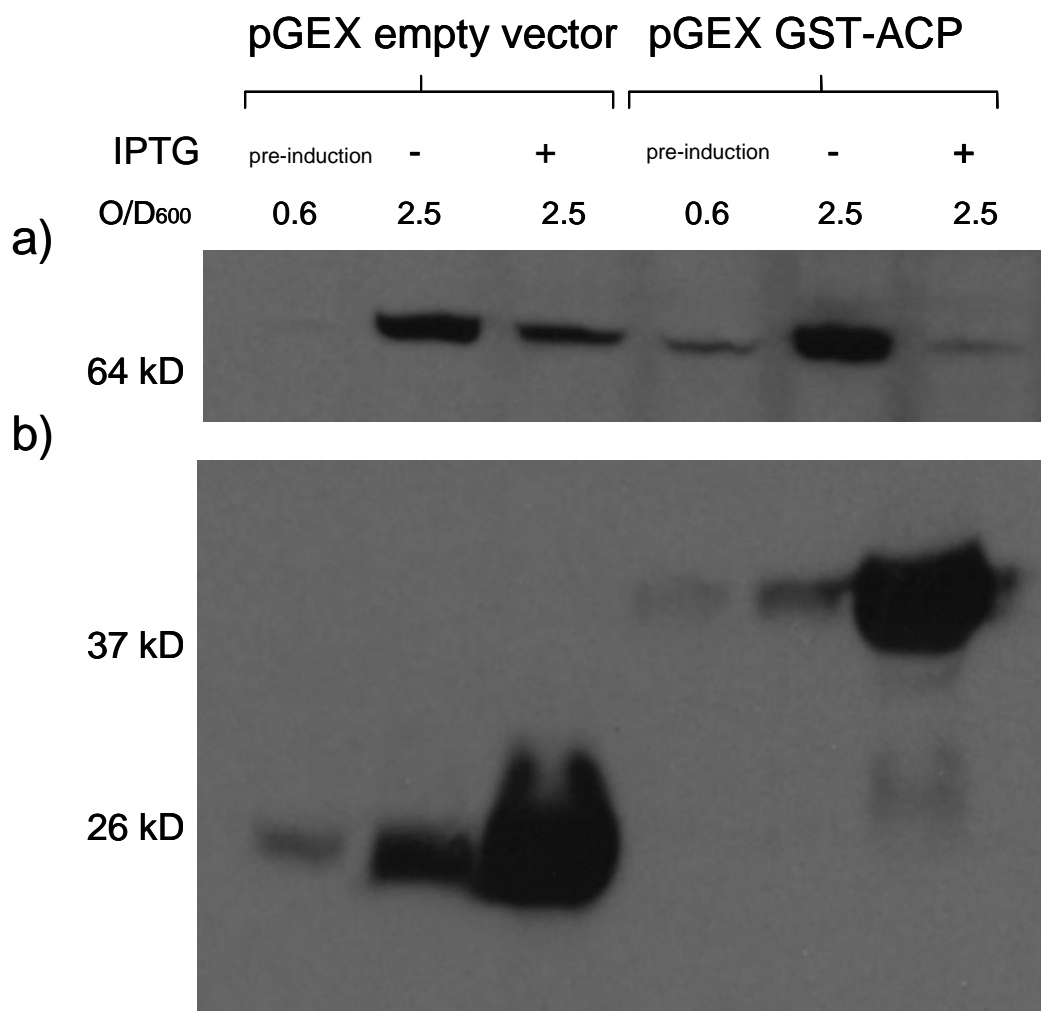
Figure 19: Effect of GST or GST-ACP expression on AidB-SPA. *E. coli* DH5α AidB-SPA cells were transformed with pGEX vectors encoding GST or GST-ACP. AidB-SPA was visualized by western blotting with anti-TAP antibodies (a) and GST and GST-ACP was visualized with anti-GST antibodies (b).
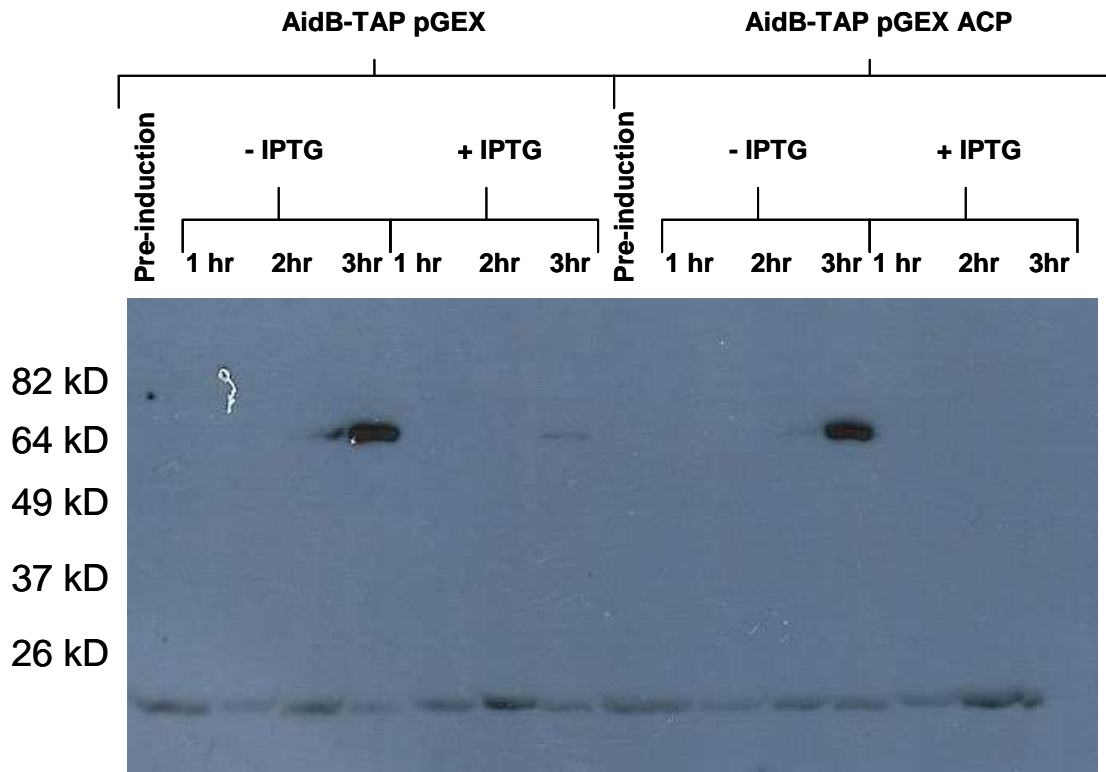
Figure 20: Growth dependent effects of GST or GST-ACP induction on AidB-SPA. *E. coli* DH5α AidB-SPA transformed with indicated pGEX plasmids were induced with IPTG at various time points. The pre-induction sample was taken at an OD of 0.6 and then the GST or GST-ACP cultures were induced with 0.2 mM IPTG. Samples of the cultures were taken after induction at one hour, two hour, or three hours, ensuring growth into stationary phase.

3. Far Western Blot Analysis of GST-ACP Binding To AidB-His$_{6x}$

Given that negligible amounts of AidB-His$_{6x}$ could be isolated and that induction of GST-ACP repressed AidB-SPA levels in the cell, a different method to examine the ACP-AidB interaction had to be explored. With only a small amount of AidB-His$_{6x}$ available, a far western blot strategy was considered (Figure 21). AidB-His$_{6x}$ as well as two controls, BSA (that has no known affinity for ACP) and *E. coli* AcpS-His$_{6x}$ (that has a high affinity for ACP), were spotted on a PVDF membrane and probed with anti-His$_{6x}$ antibodies to estimate the approximate amount of each protein spotted. Identical membrane strips were incubated with either GST-ACP or GST alone, and then washed and probed with anti-GST antibodies. Although there was some spurious detection, e.g. of the BSA control with anti-GST, the results indicate that both AidB-His$_{6x}$ and AcpS-His$_{6x}$ bind to GST-ACP but not GST. This suggests direct interaction between ACP and AidB, and appears to be a promising method for future analysis of AidB interaction with various ACP mutants.
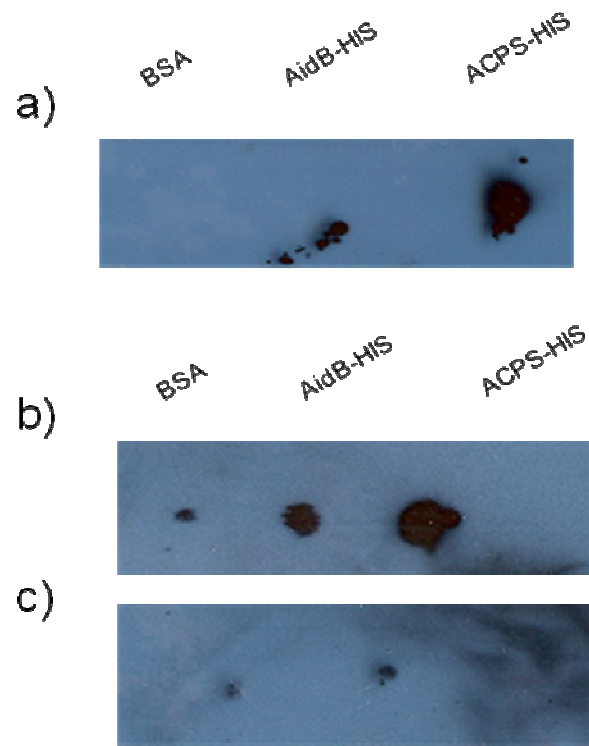
Figure 21: Far western analysis of AidB binding to ACP. AidB and controls (BSA and AcpS-His$_{6x}$) were spotted on membranes. Panel a was probed with anti-His$_{6x}$ antibodies, while panels b and c were probed with anti-GST antibodies after overnight incubation with GST-ACP or GST, respectively.

Chapter IV. Discussion

A. ACP And SpoT Interaction

In this study I found that the increased amount of SpoT co-eluting with ACP-TAP during stationary phase, identified in my earlier work, is due to an increased affinity of interaction or of availability of one or both partners. Both SpoT and ACP are constitutively expressed (Figure 9); therefore, more SpoT in the ACP-TAP purified sample suggests a greater interaction between the two proteins at this growth stage. Stationary phase is a point of low nutrient availability that is accompanied by slowed cell growth. It is in this phase of cell growth that there is an increase in the alarmone (p)ppGpp. This increase of (p)ppGpp is what alarms the cell to a lack of available nutrients and leads to growth arrest (DiRusso and Nystrom, 1998). Specifically in lipid metabolism, (p)ppGpp affects the gene expression of fabD (malonyl CoA-ACP transacylase), fabF (3-oxoacyl-ACP synthase II), fabG (3-oxoacyl-ACP reductase), and fabH (3-oxoacyl-ACP synthase III), as well as the activity of PlsB (glycerol phosphate acyl transferase), decreasing fatty acid and phospholipid synthesis, respectively (DiRusso and Nystrom, 1998). This connection to lipid metabolism suggests a possible of exchange of information about the lipid metabolic state between ACP and SpoT.

SpoT is a bifunctional protein involved in both hydrolysis and synthesis of (p)ppGpp. Throughout early and late log phase for *E. coli*, SpoT most likely exhibits its hydrolase activity, controlling the (p)ppGpp produced by its counterpart, RelA (a (p)ppGpp synthetase) and allowing the cell to continue to grow. As cells enter stationary

phase, a lack of nutrient availability and subsequent need to arrest growth causes an increase in the alarmone (p)ppGpp (DiRusso and Nystrom, 1998). This increase in (p)ppGpp is a result of the switch from hydrolase activity to synthetase activity of SpoT. This led to the belief that the increased binding of ACP to SpoT in stationary phase may be directly involved in this change in SpoT activity. ACP binds the TGS domain (Battesti and Bouveret 2006); located centrally on SpoT between the two domains controlling SpoT function. By binding SpoT, ACP could be relaying information about the cell's metabolic state, specifically a need to arrest growth, and in turn SpoT would begin to synthesize the alarmone (p)ppGpp, ultimately resulting in decreased expression and activity of FAS.

I attempted to purify His_{6x}-tagged SpoT; however, we were not able to acquire sufficient quantities to directly investigate its interaction with ACP using biophysical approaches (e.g. fluorescence) in vitro. I had similar results with a SpoT plasmid provided by Dr. Emmanuelle Bouveret (CNRS, Marseille, France), who has characterized the individual domains of SpoT but also indicated some difficulty in expressing the full length protein (E. Bouveret, personal communication). It is not uncommon to experience trouble purifying low abundance His-tagged proteins and it has been hypothesized that this may be due to the presence of metal chelators within *E. coli* lysates, in particular those found in the periplasmic space of *E. coli*. In this regard, I followed a recent procedure to purify the His_{6x}-tagged protein by subjecting the cell culture to osmotic shock to remove the periplasmic material before lysis (Magnusdottir, Johansson, et al. 2009). Unfortunately I was unable to purify any more SpoT-His_{6x} than seen with previous purification attempts. Another method that could be tried in the future to overcome the

71

difficulty in bacterial SpoT expression in vivo is in vitro transcription/translation

purification, which may result in significantly higher yield (Betton, 2004).

Nevertheless, I was successful in developing an expression system to examine SpoT-

TAP interaction using GST-tagged wild type and mutant ACPs. Transformation of

DH5α strains with pGEX plasmids encoding GST or GST-ACP fusion proteins allowed

co-expression of ACP wild type or mutants with SpoT-TAP, which was not affected by

induction of the former. Although limited in scope, my results clearly indicate that

interaction with SpoT requires a functional ACP: mutations that prevent proper folding of

the protein (F50A) or disrupt the integrity of the "recognition" helix II (SA/SB)

prevented co-purification of SpoT with ACP. This is consistent with the specificity

observed previously: SpoT binds the active holo-ACP but not apo-ACP (Battesti and

Bouveret 2006). Future work could continue using this expression system to examine

additional ACP mutants to begin to determine the specific residues involved in the

interaction, in particular the individual SA and SB mutants.

The reason for the increased interaction between ACP and SpoT in stationary phase,

and how this may regulate SpoT activity at the molecular level, still remain to be

established. One possibility is that one or both of these constitutively expressed proteins

is somehow sequestered to prevent mutual interaction until stationary phase by cellular

location or interaction with other partners, although there is no evidence to support this.

To this end, it would be interesting to observe where in the cell both individual proteins

reside in respect to one another during log phase and stationary phase growth.

A more likely possibility is that a particular modified form of ACP may accumulate

during stationary phase, altering either its affinity with SpoT or the consequences of this

interaction. I attempted to examine the acyl-ACP composition at various *E. coli* growth

stages and the nature of the ACPs bound to SpoT, but without a clean and effective ACP

antibody I was unable to detect identify the different acyl-intermediates. It would,

however, be interesting to determine whether particular acyl-ACPs bind SpoT, as it may

help to further understand what is triggering the interaction in stationary phase. This

could be accomplished using the far western technique we employed to confirm the ACP-

AidB interaction, by overlaying various acyl derivatives of GST-ACP on membranes

spotted with SpoT, followed by anti-GST antibody detection. It would also be very

interesting to examine the effect of various ACP derivatives on SpoT activity in vitro.

B. ACP And AidB Interaction

In contrast to SpoT, increased interaction of AidB with ACP appears to be due to

increased levels of the former protein during stationary phase. Current results show some

evidence for direct interaction between ACP and AidB, based on far western detection of

GST-ACP (but not GST) bound to AidB-His$_{6x}$. As with SpoT, attempts to prepare

significant amounts of AidB for in vitro interaction experiments were unsuccessful, and

the dramatic decrease in AidB expression upon GST-ACP induction prevented the

approach used for SpoT. The overexpression of GST or GST-ACP from a plasmid

promoter most likely competes with that of AidB-SPA, as AidB is not constitutively

expressed, but must be induced in parallel during stationary phase. This competition for

intrecellular resources inevitably negatively affects the levels of endogenous AidB that

can be achieved, thus preventing use of this expression system to idnetify its binding partners.

Thus, unlike for SpoT, I do not know whether ACP interaction with AidB requires ACP to be in its functional holo-form. The nature of the large positively charged DNA binding groove in AidB, coupled with its elevated pI of 8.0, certainly suggests that binding with the acidic (pI = 4.0) ACP could be electrostatic in nature. This in turn might indicate that mutant forms of ACP would still readily bind AidB, as long as the acidic nature of ACP was not grossly altered. This would also suggest that the very acidic helix II is a likely binding site for AidB, and that it may be interesting to examine whether AidB binds ACP mutants in which the acidity and integrity of helix II is disrupted, such as the SA/SB mutant.

However, a lack of 'specific' ACP-AidB binding does not rule out biological significance of this interaction. Levels of AidB seem very low (almost undetectable) during logarithmic growth and, although they increase in stationary phase, are still many fold lower than that of ACP. Relative levels could not be established due to the large variation in exposures needed to visualize both proteins on western blot (Figure 9). Thus, it is conceivable that a significant fraction of AidB could be sequestered by ACP, preventing its interaction with and protection of DNA. In preliminary experiments, we attempted to examine if the binding of ACP to AidB would impair its DNA protective qualities. When cells are exposed to the alkylating agent nitrosoguanidine (MNNG), less DNA damage occurs if AidB is overexpressed (Landini, Hajec et al. 1994). Thus, if ACP binds AidB at its DNA binding site perhaps overexpression of ACP would result in more damage to DNA during exposure to MNNG. Unfortunately, as seen in Figures 19 and 20,

the overexpression of ACP affects the endogenous levels of AidB. Thus, it would be difficult to interpret whether any increase in DNA damage during MNNG mutagenesis would be due to an increase in ACP-AidB binding or to a decrease in AidB levels.

If ACP is binding AidB at its positively charged DNA binding domain, then it is logical to question whether ACP may also interact with any of the other adaptive response proteins, Ada, AlkA and AlkB, which also bind DNA and take part in DNA repair mechanisms. We did not visualize any of these proteins either by western blotting of extracts from SPA-tagged strains, or by IDA mass spectrometry of total eluant digests after ACP-TAP or SPA purification, suggesting that they may be present at very low abundance. To see if we could identify these other adaptive response proteins in the ACP-TAP purified sample we also tried MRM, which is a more sensitive method to detect and quantify proteins known or expected to be in complex samples. In a regular IDA experiment only the most abundant and/or easily ionized peptides may be detected, while lower abundance peptides that are more challenging to ionize may be missed. Confidence in protein identification using MRM requires both that the peptide precursor(s) be specific to the protein of interest, and that multiple transitions from a precursor are overlayed on the LC gradient. Using these criteria, MRM was successful in detection of some proteins (e.g. AidB) in ACP-TAP eluates which IDA analysis did consistently identify. I also found limited evidence for AlkA and AlkB in ACP-TAP eluates (e.g. one or two transitions from a single precursor); however, these results are not conclusive. Clearly, development and optimization of MRM protocols warrant further investigation.

The verified growth dependent interactions of both AidB and SpoT with ACP are just part of a larger protein interaction network in which ACP plays a central role, and are of great interest in the search for new antibiotics. It has been suggested that the information acquired through understanding complete interaction networks for bacterial strains could be exploited for the design of broad spectrum combination therapies for drug resistance diseases (Babu, Musso et al. 2009). Both AidB and SpoT are proteins involved in the *E.coli* response to environmental stress, and thus play key roles in bacterial viability. Further understanding of these interactions will aid in the search for novel antibacterial strategies, which due to increase antibiotic resistance is of great importance.

References

Anderson, M. S. and C. R. Raetz (1987). "Biosynthesis of lipid A precursors in *Escherichia coli* a cytoplasmic acyltransferase that converts UDP-N acetylglucosamine to UDP-3-O-(R-3-hydroxymyristoyl)-N-acetylglucosamine." J Biol Chem 267: 5159-5169.

Aravind, L. and E. V. Koonin (2001). "The DNA-repair protein Alkb, EGL-9, and leprecan define new families of 2-oxoglutarate and iron-dependent dioxygenases. Genome Biol 2: RESEARCH0007.1-0007.8.

Babu, M., G. Musso, et al. (2009). "Systems-level approaches for identifying and analyzing genetic interaction networks in *Escherichia coli* and extensions to other prokaryotes." Mol Biosyst. 5:1439-1455.

Battesti, A. and E. Bouveret (2006). "Acyl carrier protein/SpoT interaction, the switch linking SpoT-dependent stress response to fatty acid metabolism." Mol Microbiol 62: 1048-1063.

Betton, J.M. (2004). "High throughput cloning and expression strategies for protein production." Biochimie 86: 601-605.

Bougdour, A. and S. Gottesman (2007). "ppGpp regulation of RpoS degradation via anti adaptor protein IraP." Proc Natl Acad Sci U S A 104: 12896-12901.

Bowles, T., A. H. Metz, et al. (2008). "Structure and DNA binding of alkylation response protein AidB." Proc Natl Acad Sci U S A 105: 15299-15304.

Brockman, H. L. and W. A. Wood (1975). "Electron-transferring flavoprotein of *Peptostreptoccus elsdenii* that functions in the reduction of acrylyl-coenzyme-A." J Bacteriol 124: 1447-1453.

Butland, G., J. M. Peregrin-Alvarez, et al. (2005). "Interaction network containing conserved and essential protein complexes in *Escherichia coli*." Nature 433: 531 537.

Byers, D. M. and H. Gong (2007). "Acyl carrier protein: structure-function relationships in a conserved multifunctional protein family." Biochem Cell Biol 85: 649-662.

Byers, D. M. and E. A. Meighen (1985). "Acyl-acyl carrier protein as a source of fatty acids for bacterial bioluminescence." Proc Natl Acad Sci U S A 82: 6085-6089.

Campbell, J. W. and J. E. Cronan (2001). "Bacterial fatty acid synthesis; tragets for antibacterial drug discovery." Annu Rev Microbiol. 55: 301-332.

Cashel, M. and D. R. Gentry (1996). "Mutational analysis of the *Escherichia coli* spoT gene identifies distinch by overlapping regions involved in ppGpp synthesis and degradation." <u>Mol Microbiol</u> 19: 1373-1384.

Chu, M., R. Mierzwa, et al. (2003). "Structure elucidation of Sch 538415, a novel acyl carrier protein synthase inhibitor from a microorganism." <u>Bioorg Med Chem Lett</u> 3: 3827-3829.

Dinglay, S., S. C. Trewick, et al. (2000). "Defective processing of methylated single stranded DNA by *E. coli* AlkB mutants." <u>Genes Dev</u> 14: 2097-2105.

DiRusso, C. C. and T. Nystrom (1998). "The fats of *Escherichia coli* during infancy and old age: regulation by global regulators, alarmones and lipid intermediates." <u>Mol Microbiol</u> 27: 1-8.

Falnes, P. O., R. F. Johansen, et al. (2002). "AlkB-mediated oxidative demethylation reverses DNA damage in *Escherichia coli*." <u>Nature</u> 419: 178-182.

Flaman, A. S., J. M. Chen, et al. (2001). "Site-directed mutagenesis of acyl carrier protein (ACP) reveals amino acid residues involved in ACP structure and acyl-ACP synthetase activity." <u>J Biol Chem</u> 276: 35934-35939.

Gaynor, E. C., D. H. Wells, et al. (2005). "The *Campylobacter jejuni* stringent reponse controls specific stress survivial and virulence-associated phenotypes." <u>Molecular Biology</u> 56(1): 8-27.

Gong, H., A. Murphy, et al. (2007). "Neutralization of acidic residues in helix II stabilizes the folded conformation of acyl carrier protein and variably alters its function with different enzymes." <u>J Biol Chem</u> 282: 4494-4503.

Gould, T. A., H. P. Schweizer, et al. (2004). "Structure of the Pseudomonas aeruginosa acyl-homoserinelactone synthase LasI." <u>Mol Microbiol</u> 53: 1135-1146.

Gropp, M., Y. Strausz, et al. (2001). "Regulation of *Escherichia coli* RelA requires oligomerization of the C-terminal domain." <u>J Bacteriol</u> 183: 570-579.

Heath, R. J., S. Jackowski, et al. (2002). <u>Fatty acid and phospholipid metabolism in prokaryotes</u>. Amsterdam, Elsevier.

Heath, R. J., S. W. White, et al. (2001). "Lipid biosynthesis as a target for antibacterial agents." <u>Prog Lipid Res</u> 40: 467-497.

Heinemeyer, E. A. and D. Richter (1977). "*In vitro* degradation of guanosine tetraphosphate (ppGpp) by an enzyme associated with the ribosomal fraction of *Escherichia coli*." <u>FEBS Lett</u> 84: 357-361.

Hernandez, V. J. and H. Bremer (1991). "*Escherichia coli* ppGpp Synthetase II Activity Requires *spoT*." J Biol Chem 266: 5991-5999.

Hollis, T., Y. Ichikawa, et al. (2000). "DNA bending and a flip-out mechanism for base excision by the helic-hairpin-helix DNA glycosylase, *Escherichia coli* AlkA." Embo J 19: 758-766.

Hollis, T., A. Lau, et al. (2001). "Crystallizing thoughts about DNA base excision repair." Prog Nucleic Acid Res Mol Biol 68: 305-314.

Hughes, C., J. P. Issartel, et al. (1992). "Activation of *Escherichia coli* prohemolysin to the membrane-targetted toxin by HlyC-directed ACP-dependent fatty acylation." FEMS Microbiol Immunol 5: 37-43.

Infectious Disease Society of America (2004). Bad Bugs, No Drugs: As Antibiotic Discovery Stagnates. A public Health Crisis Brews. Alexandria, VA, Infectious Diseases Society of America: 1-37.

Issartel, J.P., Koronakis, V., et al. (1991) "Activation of *Escherichia coli* prohaemolysin to the mature toxin by acyl carrier protein-dependent fatty acylation." Nature 351: 759-761.

Jiang, P. and J. E. Cronan, Jr. (1994). "Inhibition of fatty acid synthesis in *Escherichia coli* in the absence of phospholipid synthesis and release of inhibition by thioesterase action." J Bacteriol 176: 2814-2821.

Jones, P. J., T. A. Holak, et al. (1987). "Structural comparison of acyl carrier protein in acylated and sulfhydryl forms by two-dimensional 1H NMR spectroscopy." Biochemistry 26: 3493-3500.

Jordan, S. W. and J. E. Cronan (1997). "A new metabolic link: the acyl carrier protein of lipid synthesis donates lipoic acid to the pyruvate dehydrogenase complex in *Escherichia coli* and mitochondria." J Biol Chem 272: 17903-17906.

Keating, M. M., H. Gong, et al. (2002). "Identification of a key residue in the conformational stability of acyl carrier protein." Biochim Biophys Acta 1601: 208-214.

Kim, Y., E. L. Kovrigin, et al. (2006). "NMR studies of *Escherichia coli* acyl carrier protein: dynamic and structural differences of the apo- and holo-forms." Biochem Biophys Res Commun 341: 776-783.

Kim, Y. and J. H. Prestegard (1990). "Refinement of the NMR structures for acyl carrier protein with scalar coupling data." Proteins 8: 377-385.

Koivisto, P., T. Duncan, et al. (2003). "Minimal methylated substrate and extended substrate range of *Escherichia coli* AlkB protein, a 1-methyladenine-DNA dioxygenase." J Biol Chem 265: 14754-14762.

Labhan, J., O. D. Scharer, et al. (1996). "Structural basis for the excision repair of alkylation-damaged DNA." Cell 86: 321-329.

Landini, P., L. I. Hajec, et al. (1994). "Structure and transcriptional regulation of the *Escherichia coli* adaptive response gene aidB." J Bacteriol 176: 6583-6589.

Landini, P. and M. R. Volkert (2000). "Regulatory responses of the adaptive response to alkylation damage: a simple regulon with complex regulatory features." J Bacteriol 182: 6543-6549.

Lindahl, T., B. Sedgwick, et al. (1988). "Regulation and expression of the adaptive reponse to alkylating agents." Annu Rev Biochem 57: 133-157.

Magnusdottir, A., I. Johansson, et al. (2009). "Enabling IMAC purification of low abundance recombinant proteins from *E.coli* lysates." Nat Methods 6: 477-478.

Mechold, U., H. Murphy, et al. (2002). "Intramolecular regulation of the opposing (p)ppGpp catalytic activities of Rel(Seq), the Rel/Spo enzymes from *Streptococous equismitis*." J Bacteriol 184: 2878-2888.

Nakabeppu, Y. and M. Sekiguchi (1986). "Regulatory mechanisms for induction of synthesis of repair enzymes in response to alkylating agents: Ada protein acts as a transcriptional regulator." Proc Natl Acad Sci U S A 83: 6297-6301.

Nieminuszczy, J. and E. Grzesiuk (2007). "Bacterial DNA repair genes and their eukaryotic homologues: 3. AlkB dioxygenase and Ada methyltransferase in the direct repair of alkylated DNA." Acta Biochim Pol 54: 459-468.

Parris, K. D., L. Lin, et al. (2000). "Crystal structures of substrate binding to *Bacillus subtilis* holo-(acyl carrier protein) synthase reveal a novel trimeric arrangement of molecules resulting in three active sites." Structure 8: 883-95.

Paul, B. J., M. M. Barker, et al. (2004). "DskA: a critical component of the transcription initiation machinery that potentiates the regulation of rRNA promoters by ppGpp and initating NTP." Cell 118: 311-322.

Pinner, R. W., S. M. Teutsch, et al. (1996). "Trends in infectious diseases mortality in the United States." JAMA 275: 189-193.

Potrykus, K. and M. Cashel (2008). "(p)ppGpp: still magical?" Annu Rev Microbiol. 62: 34-51.

Powers, J. H. (2004). "Antimicrobial drug development--the past, the present, and the future." <u>Clin Microbiol Infect</u> 10: 23-31.

Rock, C. O. and J. E. Cronan (1996). "*Escherichia coli* as a model for the regulation of dissociable (type II) fatty acid biosynthesis." <u>Biochem Biophys Acta</u> 1302: 1-16.

Rock, C. O. and S. Jackowski (1982). "Regulation of phospholipid synthesis in *Escherichia coli*. Composition of the acyl-acyl carrier protein pool in vivo." <u>J Biol Chem</u> 257: 10759-10765.

Rohankhedkar, M. S., S. B. Mulrooney, et al. (2006). "The AidB component of the *Escherichia coli* adaptive response to alkylating agents is a flavin-containing, DNA-binding protein." <u>J Bacteriol</u> 188: 223-230.

Roujeinikova, A., C. Baldock, et al. (2002). "Crystallization and preliminary X-ray crystallographic studies on acyl-(acyl carrier protein) from *Escherichia coli*." <u>Acta Crystallogr D Biol Crystallogr</u> 58: 330-332.

Samson, L. and J. Cairns (1977). "A new pathway for DNA repair in *Escherichia coli*." <u>Nature</u> 267: 281-283.

Sarubbi, E., K. E. Rudd, et al. (1989). "Characterization of the *spoT* gene in *Escherichia coli*." <u>J Biol Chem</u> 264: 15074-15082.

Sedgwick, B. (2004). "Repairing DNA-methylation damage." <u>Nat Rev</u> 5: 148-157.

Sedgwick, B. and T. Lindahl (2002). "Recent progress on the Ada response for inducible repair of DNA alkylation damage." <u>Oncogene</u> 21: 8886-8894.

Seyfzadeh, M., J. Keener, et al. (1993). "*spoT*-dependent accumulation of guanosine tetraphosphate in response to fatty acid stravation in *Escherichia coli*." <u>Proc Natl Acad Sci U S A</u> 90: 11004-11008.

Shorr, A. F. (2009). "Review of studies on the impact on Gram-negative bacterial resistance on the outcomes in the intensive care unit." <u>Crit Care Med</u> 37: 1463-1469.

Slama, T. G. (2008). "Gram-negative antibiotic resistance: there is a price to pay." <u>Crit Care</u> 12: 1-7.

Smith, S., A. Witkowski, et al. (2003). "Structural and functional organization of animal fatty acid synthase." <u>Prog Lipid Res</u> 42: 289-317.

Spellberg, B., J. H. Powers, et al. (2004). "Trends in anitmicrobial drug development: implications for the future." <u>Clin Infect Dis</u> 38: 1279-1286.

Tener, D. M. and K. H. Mayo (1990). "Divalent cation binding to reduced and octanoyl acyl-carrier protein." Eur J Biochem 189: 559-565.

Teo, I., B. Sedgwick, et al. (1984). "Induction of resistance to alkylating agents in *E. coli:* the ada+ gene product serves both as a regulatory protein and as an enzyme for repair of mutagenic damage." Embo J 3: 2151-2117.

Therisod, H., A. C. Weissborn, et al. (1986). "An essential function for acyl carrier protein in the biosynthesis of membrane-derived oligosaccharides of *Escherichia coli*." Proc Natl Acad Sci U S A 83: 7236-7240.

Thomas, J., D. J. Rigden, et al. (2007). "Acyl carrier protein phosphodiesterase (AcpH) of *Escherichia coli* is a non-canonical member of the HD phosphatase/phosphodiesterase family." Biochemistry 46: 129-136.

Volkert, M. R., D. C. Nguyen, et al. (1986). "*Escherichia coli* gene induction by alkylation treatment." Genetics 112: 11-26.

Wells, D. H. and E. C. Gaynor (2006). "*Helicpbacter pylori* Initiates the stringent response upon nutrient and pH downshift." Journal of Bacteriology 188: 3726 -3729.

Wendrich, T. M., G. Blaha, et al. (2002). "Dissection of the mechanism for the stringent factor RelA." Mol Cell 10: 779-788.

White, S. W., J. Zheng, et al. (2005). "The structural biology of type II fatty acid biosynthesis." Annu Rev Biochem 74: 791-883.

Wolf, Y. I., L. Aravind, et al. (1999). "Evolution of aminoacyl-tRNA synthetase - analysis of unique domain architectures and phylogenetic trees reveals a complex history of horizantal gene transfer events." Genome Res 9: 680-710.

Wright, P. E. and H. J. Dyson (1999). "Intrinsically unstructured proteins: re-assessing the protein structure-function paradigm." J Mol Biol 293: 321-331.

Wright, T. H. and K. A. Reynolds (2007). "Antibacterial targets in fatty acid biosynthesis." Current Opinion in Microbiology 10: 447-453.

Xiao, H., M. Kalman, et al. (1991) "Residual guanosine 3',5'-bispyrophosphate synthetic activity of relA null mutants can be eliminated by spoT null mutants." J Biol Chem 266: 5980-5990.

Zhang, Y. M., M. S. Rao, et al. (2001). "Identification and analysis of the acyl carrier protein (ACP) docking site on beta-ketoacyl-ACP synthase III." J Biol Chem 276: 8231-8238.

Zhang, Y. M., S. W. White, et al. (2006). "Inhibiting bacterial fatty acid synthesis." <u>J Biol Chem</u> 281: 17541-17544.

Zhang, Y. M., B. Wu, et al. (2003). "Key residues responsible for acyl carrier protein and beta-ketoacyl-acyl carrier protein reductase (FabG) interaction." <u>J Biol Chem</u> 278: 52935-52943.